International Journal of Concrete Structures and Materials

RESEARCH

Open Access

The Effect of Different Types of Fibers and Cement Substitutes on High-Performance Concrete Cured in Standard, Thermal, and Sulfate Conditions

Shiva Safari Taleghani[1], Amir Masoud Salehi[1], Mojtaba Mehraein[1*] and Gholamreza Asadollahfardi[1]

Abstract

In this study, the workability and mechanical characteristics of concrete containing different types of fibers and cement substitutes of concrete under standard, thermal, and sulfate environment curing conditions were compared. Normal concrete was made with a water-to-cement ratio of 0.43, and high-performance concrete was produced with smaller water-to-cement ratios (0.38, 0.33, and 0.28). Macro steel fibers in three different amounts and with two length sizes (60 mm and 30 mm), including polypropylene fibers (PP), and high-performance polypropylene fibers (HPP) in combination with steel fibers, blast furnace slag, and silica fume were used as cement substitutes. The tests performed include slump tests, compressive, flexural strength, and Brazilian tensile and microstructure images. Results showed that thermal curing (without moisture) reduces compressive, tensile, and flexural strength compared to standard curing conditions, and using the steel fibers this weakness was not reduced. In standard curing, by adding steel fibers, the mechanical properties increase significantly, and by increasing the percentage of steel fibers, the mechanical properties also improve. Concretes with a combination of different types of fibers did not favorably affect the mechanical properties of concrete compared to steel fiber concretes.

Keywords High-performance concrete (HPC); fibers, Supplementary cementitious materials, Thermal curing, Sulfate attack

1 Introduction

The American Concrete Institute (ACI) defines high-performance concrete (HPC) as concrete that exhibits enhanced workability, mechanical properties, or durability when compared to standard concrete (Russell, 1999). This type of concrete typically features a low water-to-cement ratio (less than 0.35), high-quality aggregates, a substantial cement content (450–550 kg/m^3), the inclusion of silica fume (5–15% of the cement's weight), and a superplasticizer (Afroughsabet, 2020). In addition, in high-performance concrete (HPC), increasing the significant proportion of cement and incorporating mineral additives can significantly enhance the properties of the concrete. However, this may also lead to increased susceptibility to premature cracking, which can reduce the service life of concrete structures. The application of fibers is an appropriate solution to overcome this weakness, and by preventing crack propagation, it produces a material with high tensile, flexural strength, plasticity, and energy absorption (Afroughsabet et al., 2016).

In recent years, the construction industry has seen a rise in the use of an innovative technology known as high-performance fiber-reinforced concrete (HPFRC). The desired characteristics influence the materials

Journal information: ISSN 1976-0485 / eISSN 2234-1315.

*Correspondence:
Mojtaba Mehraein
mehraein@khu.ac.ir
[1] Faculty of Engineering, Kharazmi University, Tehran, Iran

chosen for HPFRC, and the local economy determines the availability of appropriate alternative materials. Fibers can be added to cement concrete to enhance its tensile strength, ductility, toughness, and durability. The HPFRC is a specialized form of HPC designed to improve concrete quality in several aspects. It achieves this by employing a low water-to-cement ratio, incorporating pozzolanic materials as replacements, and adding fibers. The most important effect of fibers is the capability to delay the propagation of cracks in concrete. Fibers can be categorized as metallic, polymeric, or natural. Of these, steel fibers (metallic) are the most commonly utilized for both structural and non-structural applications (Gu et al., 2016).

The properties of high-performance concrete are meaningfully affected by the preparation process, especially the curing conditions. Due to the exceptional quality of high-performance concrete, steam curing is commonly employed as an effective curing method (Li et al., 2020a). Although steam curing provides high mechanical properties and durability at an early age, in the long term, it may have an adverse impact on the performance of concrete, since the high temperature accelerates the hydration of cement materials, which accelerates the distribution of heterogeneous hydration products and possibly the formation of a relatively looser structure and more porosity. Similarly, acceleration of hydration by processing at high temperatures in some cases causes a delay in the formation of ettringite (Shen et al., 2019; Shin & Yoo, 2020).

Several researchers have studied using different fibers in HPC, such as Yu et al. (2014a), which indicated that the addition of microsteel fibers negatively affects the workability of concrete. They observed that as the proportion of steel fibers increased from 0.5 to 2.5% of the concrete volume, the slump decreased. Li et al. (2024) concluded that steel fibers are basically added to concrete to increase flexural properties. However, the increase in flexural strength depends on the type of concrete, type of fibers, and size, which leads to different growth rates of flexural strength. On the other hand, Bolkbache et al. (2010a) revealed that when fiber-reinforced concrete does not have sufficient workability, it reduces the effect of fibers on the mechanical performance of concrete. In a study of two metal fibers with two different sizes, Wu et al. (2019a) concluded that metal fibers with longer lengths are more effective in growing compressive strength. However, the combination of two fibers in two lengths, short and long, is more effective in controlling crack propagation. Aiamsri et al. (2024) investigated the bond strength in conventional concrete and high-performance concrete with steel fibers. They found that the bond strength increased with increasing compressive strength of concrete.

Li et al. (2020b) concluded that with the increase in the amount of steel fibers, the value of the tensile strength is enhanced. They also verified the relationship between the increase in the steel fibers and the strain rate in high-performance steel fiber-reinforced concrete (HPSFRC) using the theory of energy conversion. In other studies on the effect of two types of steel fibers (smooth and sinusoidal) on microcracks, Shin and Yoo (2020) found that concrete reinforced with sinusoidal fibers is more vulnerable to corrosion than concrete reinforced with smooth fibers, which was determined by the earlier deterioration of tensile performance. In examining the volume of steel fibers used in concrete, the effect of a volume of steel fibers of 0.5–1.5% leads to a 43% increase in maximum failure load capacity and a 165% increase in displacement between frames compared to samples with fewer fibers (Maglad et al., 2023). Various researchers have proposed the combined use of different types of fibers, including steel fibers and synthetic fibers, in high-performance concrete to improve its performance (Li et al., 2019; Wang & Guo, 2018; Yoo & Kim, 2019). Typically, incorporating a combination of metal fibers and polypropylene into reinforced concrete significantly enhances its resistance to cracking across various dimensions and locations (Wang et al., 2023).

Xei et al. (2018) studied the characteristics of self-shrinkage and drying shrinkage of ultra-high-performance concrete (UHPC). They found that porosity and the amount of unreacted paste material are the two factors that affect the shrinkage characteristics of UHPC. They replaced half of the mixed water with crushed ice to reduce self-shrinkage. One of the typical applications of fibers is to reduce cracking in concrete due to shrinkage and thermal variations. Accordingly, fibers can also improve durability (Abdi Moghadam & Izadifard, 2021; Nogueira et al., 2021; Shen et al., 2022). Shen et al. (2019) used double-ended steel fibers to find the effects on the cracking potential of concrete in ring samples. They found that the cracking potential and residual stress decreased with an increase in the volume of double hooked-ended steel fibers. Lv et al. (2021) found that as steel fibers undergo corrosion, their capacity to control cracks diminishes, leading to a rapid increase in crack width.

Shen et al. (2019) also studied the effect of different heat curing on various properties of reinforced concrete. They emphasized that heat curing with steam with and without pressure improves the mechanical properties and durability of concrete. Lessly et al. (2020) examined the flexural characteristics of reinforced concrete incorporating supplementary cementitious materials (SCMs) under various curing conditions. They discovered that using hot water and steam during curing significantly improved

the compressive and flexural characteristics in comparison with standard curing methods of the same duration. Helmi et al. (2016) studied the impact of high-pressure steam curing on concrete microstructure development. They discovered that the curing process, involving thermal expansion of solid phases, volumetric air expansion, and increased pressure in voids, accelerates the diffusion rate of fine cracks formed during shrinkage. Crystalline hydrate is primarily formed within the network of narrow capillary pores.

Matar and Assaad (2019) investigated various SCC mixtures and polypropylene fibers (PPF), in different ratios of water-to-cement conditions. They found that adding PPF significantly decreases the rheological characteristics and passing ability of SCC, especially for the mixes containing higher rates of replaced RCA. Matar and Zéhil (2019) investigated a mixture of recycled concrete aggregates and PPF in concrete. Using PPF, the compressive strength and the density of the concrete did not change significantly. In addition, the modulus of elasticity of concrete and the Poisson's ratio of concrete marginally decreased using PPF.

Chen et al. (2023) studied the combination impacts of using recycled tire polymer fiber and steel fiber on concrete characteristics. They found that by adding the fibers, the workability of the concrete decreased. However, increasing the fibers improved the flexural toughness of the concrete and the average strength of the concrete. A combination of glass fiber and polypropylene fiber was used by Hadeed et al. (2023) to produce lightweight concrete (LWC) and high-strength concrete (HSC). They found that using glass fiber (GF), the flexural strength, compressive strength, and splitting tensile strength of the samples increased notably. Sharma and Senthil (2023) found that the workability of the sample decreased using synergic consumption of manufactured sand and recycled coarse aggregates. Antarvedi et al. (2023) utilized two varieties of steel fibers (crimped steel fiber and hooked-end steel fiber), each separately combined with polypropylene fibers in concrete. Results showed that the steel fibers increased flexural strength characteristics. In addition, the steel fibers decreased the crack propagation. Hosseinzadeh et al. used different types of fiber in normal concrete and HPC curing in standard conditions. The addition of fibers reduces the workability of concrete. Incorporating 0.5% polypropylene fiber enhances the compressive and tensile strength of the concrete. In addition, lowering the water–cement ratio (w/c) decreases the concrete's water absorption (Hosseinzadeh et al., 2023).

Most research on fiber-reinforced concrete focuses on the influence of fiber types on the mechanical properties of the concrete cured under standard conditions. However, in practical applications, curing often occurs in environments with high temperatures or exposure to aggressive sulfate ions. This study aims to address the impact of these challenging curing conditions and environments, a topic that has received limited attention in previous research. In this study, the effects of using steel fibers on the workability and mechanical characteristics of high-performance concrete (HPC) were determined. Another objective of this study is to clarify the impact of combining steel fibers with PP fibers and HPP fibers on the mechanical properties of HPC. In addition, the effects of thermal curing, curing in a sulfated environment, and the use of silica fume on the mechanical characteristics of HPC were determined.

2 Materials and Methods

2.1 Materials

The characteristics of the cement are presented in Tables 1 and 2. Type 2 Portland cement sourced from Abyek, Qazvin, Iran, was used, meeting the requirements of the ASTM C150/C150M (ASTM C150 & C150M-18, 2018) standard. Table 1 also indicates silica fume properties. The silica fume is light gray. The specific gravity and the relative density of silica fume are 250 g/cm^3 and 2.21, respectively.

The maximum size of coarse aggregate and sand aggregate were 9 mm and 4.75 mm, respectively. The coarse aggregate used in this research consists of 50% crushed river gravel and 50% natural aggregate. The aggregated was prepared from Hashgard Mine 11. A sieve analysis (ASTM C136-84) of fine and coarse aggregate is presented in Fig. 1. (ASTM C136–84a, 1984). The density of the polycarboxylate-based superplasticizer is 1.1 ± 0.02 g/cm^3 at 20°C. The company producing superplasticizers is Shimi Sakhteman Company. The increase in concrete air content due to the use of this superplasticizer is less than 2%.

Two types of macro steel fibers, available in two different lengths, were utilized, featuring both long and short variations. In addition, macro-polypropylene fibers were combined with other fibers. These fibers were prepared by Sirjan Yarn and Granule Company (Table 3). High-performance polypropylene fibers (HPP) are a new type of fiber with high efficiency in concrete. These fibers are also prepared by Sirjan Yarn and Granule Company (Fig. 2).

2.2 Concrete Mix Designs

Table 4 indicates the 22 samples with different concrete mix designs. The national concrete mixture design of Iran (Mesbah Irandoost & S. A., 2010) was utilized to achieve the design of the final mixes. Two w/c ratios of 0.43 and 0.38 were considered for obtaining ordinary and high-performance concrete. Likewise,

Table 1 Chemical characteristics of silica fume and cement

Chemical compound	Portland cement	ASTM C150/C150M (ASTM C150 & C150M-18, 2018) Limits	Silica fume	ASTM C1240 (ASTM C, 1240. 2003) Limits
	%			
SiO_2	27.52	Min 20	93.6	90–95
Al_2O_3	1.58	Max 6	0.8	0.6–1.2
Fe_2O_3	6.68	Max 6	0.87	0.3–1.3
CaO	82.26		0.5	0.5–1.5
MgO	6.62	Max 5	0.97	0.5–2
SO_3	9.62	Max 3	–	–
Na_2O	7.65		0.5	0.3–0.5
K_2O	7.86		0.4	0.2–0.5
Insoluble residue	0.69	Max 0.75	–	–
C	–		0.3	0.2–0.4
S	–	ISIRI389 (Matar & Assaad, 2019)	0.05	0.04–0.08
MnO	–	Min 20	0.06	0.02–0.07
P_2O_5	–	Max 6	0.03	0.04
LOI	–	Max 6	2	0.4–3
pH	–		7	6.8–8

Table 2 Cement's physical characteristics

Characteristic	Results	ASTM C 150/C 150M –09 (ASTM C150 & C150M-18, 2018) limits
Longitudinal expansion (%)	0.21	Max 0.8
Fineness (Blain) (cm^2/kg)	3081	Min 2800
Retained on a 90-micron sieve (%)	5.7	
Water percentage (%)	23	
Initial setting time (min)	153	Min 45 (min)
Secondary setting time (min)	212	Max 6 (hrs)
Compressive strength at 2 days (kg/cm^2)	160	–
Compressive strength at 3 days (kg/cm^2)	208	Min 100

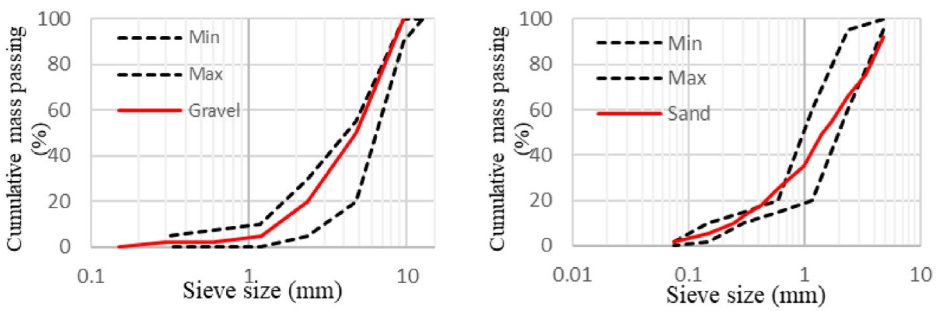

Fig. 1 Sieve analysis: **a** coarse and **b** fine

Table 3 Characteristics of fibers

Specification	Steel fiber with two hooks-ends	Polypropylene fibers	High-performance Polypropylene *Fiber*
Special weight (kg/m^3)	7850	0.91	0.91
Diameter (mm)	0.8	0.035	0.4
Length (mm)	3050	12	50
Modulus of elasticity (*GPa)*	205	3–3.5	6.0
Tensile strength (MPa)	1100	350–400	500–600
Color		White	white

(a) (b) (c)

Fig. 2 Fibers **a** steel; **b** polypropylene; **c** high-performance polypropylene fibers

due to the desired workability, which is also affected by the use of fibers, a proportion of sand 60% and gravel 40% was used to achieve a uniform paste. Three different percentages of steel fiber were used: 1, 1.5, and 2%. Since better results were obtained with 1.5% fiber, this percentage of fibers was used as a fixed percentage. In addition, polypropylene and HPP fibers were used in combination with steel fibers, and the selection of the percentages of these two types of fibers was based on the manufacturer's recommendation and previous research (Antarvedi & Banjara, 2023).

In Table 4, the samples are coded in such a way that the control sample is marked with the letter C, and the w/c of each design is next to its name, St is added to the samples with steel fibers, and the number in front of St shows the percentage of fibers, and SF is added to the samples with silica fume. The number in front of SF indicates the silica fume percentage, and the samples with slag are identified by adding letters G. Again, the number in front of the letters G describes the percentage of slag used. Likewise, samples with PP and HPP fibers are shown with the addition of these letters. In addition, in the test results and analysis, heat-cured samples indicate the CH symbol.

2.3 Test Procedure and Curing Conditions

The slump test based on ASTM C143/C143M-20 standard was done to determine the workability of concrete (ASTM C143 & C143M-20, 2020). Nine cube samples of 100×100×100 mm for ages 7, 28, and 90 were used by BS EN 12390-3:2019 were used to test the compressive strength of concrete (BSEN, 2019). 300×150 mm cylindrical molds at 28 days, ASTM C496-17 (ASTMC496, 2017) standard, were used to test the tensile strength. For the flexural strength experiment at 28 days, prismatic molds measuring 400×100×100 mm were used in accordance with the ASTM C1609-19a standard (ASTM C, 1609, C1609M-19a 2019). In all experiments, three series of samples were tested for each age.

Three types of concrete curing, including Standard curing according to ASTM C192/C192M-19 (ASTM C192., 2019), thermal curing, and sodium sulfate environment curing, were carried out by ASTM C 1012-04 (ASTM C, 1012. 1012).

Thermal curing clarified the effect of heat on the fresh and hardened mechanical properties of concrete as simulated samples of bulk concrete or curing concrete on thermal conditions and compared it with standard curing samples. In addition, the curing of concrete

Table 4 22 concretes mix design

Code of samples	W/B	Water kg/m^3	Cement	Silica fume	Slag	Sand	Gravel	Steel fiber %[3]	PP[1]	HPP fiber	SP[2] %[4]
C0.43*	0.43	193.5	450	0	0	1027	684	0	0	0	0.4
C0.43 + St1.5	0.43	193.5	450	0	0	1027	684	1.5	0	0	0.6
C0.38*	O.38	182.4	480	0	0	1029	686	0	0	0	0.6
C0.38 + St1.5	0.38	182.4	480	0	0	1029	686	1.5	0	0	0.9
C0.33*	0.33	168.3	510	0	0	1037	691	0	0	0	0.7
C0.33 + St1.5	0.33	168.3	510	0	0	1037	691	1.5	0	0	1
C0.28*	0.28	170.8	610	0	0	982	654	0	0	0	1.3
C0.28 + St1	0.28	170.8	610	0	0	982	654	1.5	0	0	1.4
C0.28 + St1.5	0.28	170.8	610	0	0	982	654	1.5	0	0	1.5
C0.28 + St2	0.28	170.8	610	0	0	982	654	2	0	0	1.8
C0.28 + St1.5 + SF20	0.28	170.8	488	122	0	955	637	1.5	0	0	1.3
C0.28 + St1.5 + SF20 + G30	0.28	170.8	305	122	183	942	628	1.5	0	0	1
C0.28 + St1.5 + SF20 + G50	0.28	170.8	183	122	305	933	622	1.5	0	0	0.9
C0.28 + SSt1.5	0.28	170.8	610	0	0	982	654	1.5	0	0	1.6
C0.28 + St0.75 + PP0.15*	0.28	170.8	610	0	0	982	654	0.75	0.15	0	1.9
C0.28 + St1 + PP0.1	0.28	170.8	610	0	0	982	654	1	0.1	0	1.7
C0.28-St1.5PP0.2*	0.28	170.8	610	0	0	982	654	1	0.2	0	2
HPP0.5*	0.28	170.8	610	0	0	982	654	0	0	0.5	1
HPP1*	0.28	170.8	610	0	0	982	654	0	0	1	1.5
HPP0.5 + St1*	0.28	170.8	610	0	0	982	654	1	0	0.5	1.1
HPP0.5 + PP0.2*	0.28	170.8	610	0	0	982	654	0	0.2	0.5	1.5
HPP0.5 + St1 + PP0.2*	0.28	170.8	610	0	0	982	654	1	0.2	0.5	1.7

1. Polypropylene fiber

2. Superplasticizer

3. Percent of concrete volume

4. percent of binder content (weight)

*The experiments were reported by Hosseinzadeh et al. (2023) (Abdi Moghadam & Izadifard, 2021)

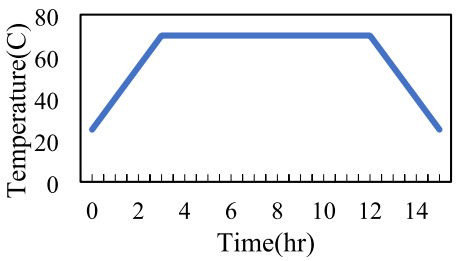

Fig. 3 Heat curing regime of concretes

samples in the presence of sodium sulfate simulates the conditions of exposure of concrete to harmful chemical environments, including environments containing sulfate ions. In the standard curing process, the samples were removed from the mold after 24 h and then cured in a tank of tap water maintained at a temperature of 22 ± 3 degrees Celsius. In curing concrete under temperature (according to Fig. 3), after casting, the samples are cured for 2 h at ambient temperature. After proper moisture insulation of the samples, the curing temperature reached 70 °C from 25 °C with a temperature gradient of 15 °C per hour for 3 h. It was cured at 70 °C for 8 h, and then at the same slope, the samples reached a temperature of 25 °C within 3 h. For the sulfate curing condition, the concretes were immersed in an aqueous environment with a 5% sodium sulfate concentration for 365 days after taking the cast.

A scanning electron microscope (SEM) was done according to the ASTM C1723-2016 (C-16 A., 2016) standard. The age of the samples was 28 days. The core of the samples was removed in such a way that the concrete sample would not be severely damaged for testing, and it was sent to the Rayan Rostak radiation laboratory in Tehran. In addition, the XRD test was conducted in accordance with ASTM E1621/E1621M (ASTM E, 1621–13 2013).

Table 5 Slump test results of different concrete mix designs

Sample code	W/B	*SP%*	*Slump(mm)*
C0.43	0.43	0.4	200 ± 2
C0.43 + St1.5	0.43	0.6	200 ± 2
C0.38	0.38	0.6	175 ± 2
C0.38 + St1.5	0.38	0.9	175 ± 2
C0.33	0.33	0.7	165 ± 2
C0.33 + St1.5	0.33	1	165 ± 2
C0.28	0.28	1.3	140 ± 2
C0.28 + St1	0.28	1.4	140 ± 2
C0.28 + St1.5	0.28	1.5	140 ± 2
C0.28 + St2	0.28	1.8	140 ± 2
C0.28 + St1.5 + SF20	0.28	1.3	140 ± 2
C0.28 + St1.5 + SF20 + G30	0.28	1	140 ± 2
C0.28 + St1.5 + SF20 + G50	0.28	0.9	140 ± 2
C0.28 + SSt1.5	0.28	1.6	140 ± 2
C0.28 + St0.75 + PP0.15	0.28	1.9	130 ± 2
C0.28 + St1.5 + PP0.1	0.28	1.7	130 ± 2
C0.28-St1.5PP0.2	0.28	2	130 ± 2
HPP0.5	0.28	1	150 ± 2
HPP1	0.28	1.5	150 ± 2
HPP0.5 + St1	0.28	1.1	150 ± 2
HPP0.5 + PP0.2	0.28	1.5	150 ± 2
HPP0.5 + St1 + PP0.2	0.28	1.7	150 ± 2

3 Results and Discussion

3.1 Fresh Properties of Concretes

Table 5 presents the result of the slump test under standard curing. The volume of superplasticizers (SPs) was added to the concretes in such a way that the concretes had the same slump with the same ratio of water to cement. The incorporation of steel fibers in all concrete samples with w/c = 0.43, 0.38, 0.33, and 0.28 required a higher dosage of superplasticizer to achieve the same slump consistency.

Therefore, the use of steel fibers decreased the workability of the concrete. Yu et al. (2014b) also found that macro steel fibers decreased the slump of concrete. The result of this study is in line with the results of Edigton et al. (1974).

For w/c = 0.28, for the samples with silica fume and slag, a smaller amount of superplasticizer was used to achieve an equal slump as compared to the control sample and the sample with steel fibers. Several studies have indicated (Boulekbache et al., 2010b; Richard & Cheyrezy, 1995) that using the silica fume in HSC, the workability of the samples improved. Other research revealed that in HSC, using a significant amount of silica fume and cement, the viscosity of the mixture increased (Wu et al., 2019b). In addition, the lowest slump amount was obtained in the composite samples containing PP fibers. Therefore, based on the results of the present study, in general, the use of fibers reduces workability, which requires the use of more superplasticizers to compensate for the reduction in workability.

3.2 Mechanical Properties of Concretes in Standard Curing

3.2.1 Compressive Strength

Fig. 4 shows the compressive strength of concrete samples with different w/c (0.43, 0.38, and 0.33). In this figure, the samples contained 1.5% steel fibers cured under standard conditions. The compressive strength increased using the steel fibers in the samples. It is more evident in low-age (7 and 28 days) samples. By increasing the age of the sample to 90 days, the difference between the compressive strength of concrete containing steel fibers and without fibers decreases. It is due to the effects of the fibers in delaying the propagation and formation of cracks (Ibrahim et al., 2017; Yu et al., 2014b). At w/c = 0.38, the 28-day compressive strength of the sample with fibers is 27% higher than that of the control sample. Many studies indicated that the steel fibers increased the compressive strength of HSC (Jin et al., 2018; Yu et al., 2014b). At w/c = 0.33, using steel fibers, the compressive strength of 7-day samples increased by 42% compared to the control sample. However, using the fiber increased the 28-day compressive strength of the sample by 8% compared to the control sample. Another noteworthy point is that in the lowest w/c (0.33), the effect of using fibers decreased in comparison with the higher w/c samples.

Fig. 5 indicates the compressive strength for w/c = 0.28, and different ratios of fibers. Increasing the percentage of fibers leads to an increase in compressive strength. For example, the 7-day compressive strength of the sample containing 1.5% steel fibers is 14% greater than the sample with 1% fibers. Similarly, the compressive strength of the sample with 2% steel fibers is 3.5% higher than the sample with 1.5% fibers and 22% more than the sample with 1% fibers.

Considering the compressive strength results, the difference with the sample with 1.5% fibers is not noticeable, and by increasing the fibers the concrete workability decreases. Hence, to reach a slump equal to the percentage of lower fibers, more superplasticizer is needed. The use of this volume of fibers is not justified economically, and the C0.28 + St1.5 sample was selected as the optimal sample. As indicated in Fig. 5, SCMs, including silica fume and slag, were also used in fiber concrete with a w/c = 0.28. In concrete with 20% silica fume powder, the compressive strength of 7 days is 2% greater than the strength of the fibrous sample without silica fume and 20% greater than the control sample. However, the 28-day compressive strength of this sample is 26 and 57% larger than the fiber sample

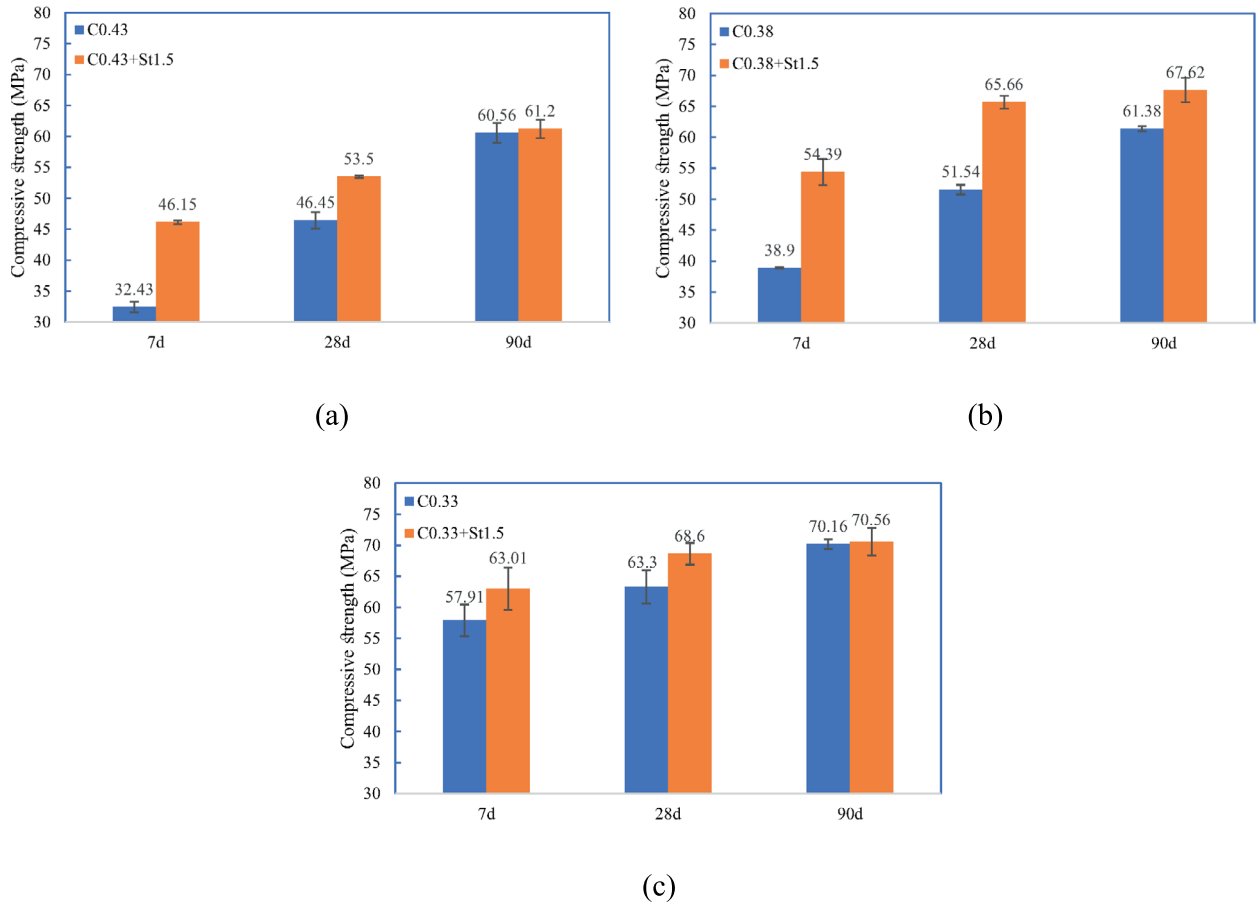

Fig. 4 Compressive strengths in W/C of 0.43, 0.38, and 0.33 with and without steel fibers (1.5%), **a** C0.43; **b** C0.38; **c** C0.33

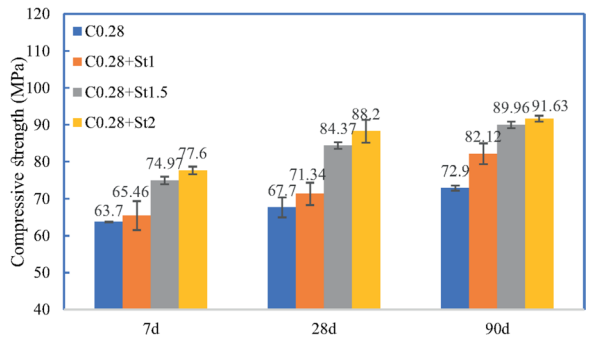

Fig. 5 Compressive strength in w/c = 0.28

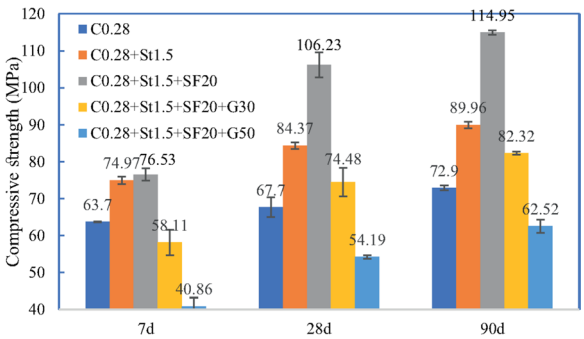

Fig. 6 Compressive strength in w/c = 0.28 with silica fume and slag with without steel fiber

without silica fume and the control sample without fiber and silica fume, respectively. Based on extensive research, substituting silica fume, a highly effective pozzolan, leads to the transformation of $Ca(OH)_2$ compounds into CSH, thereby decreasing concrete porosity and enhancing the fibers–matrix bond (Chan & Chu, 2004; Wu et al., 2016) leading to increases in the compressive strength of concrete.

The results of concretes containing silica fume and slag (C0.28 + St1.5 + SF20 + G30 and C0.28 + St1.5 + SF20 + G50) (Fig. 6) indicate that using slag as a substitute reduces the compressive strength so that replacing 30% of slag with 20% of silica fume reduced the compressive strength by 25% in comparison with the fiber sample with silica fume, 22% of the fiber sample,

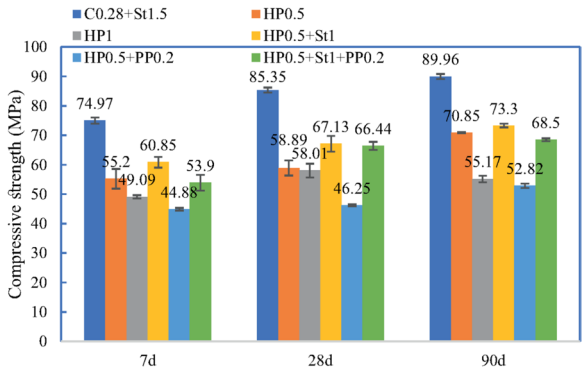

Fig. 7 Compressive strength in w/c = 0.28 containing short steel fibers and the combination of steel fibers and PP

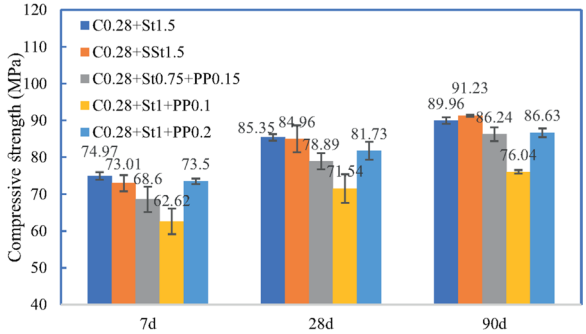

Fig. 8 Compressive strength in w/c = 0.28 containing composite fibers

and 10% of the control sample at 7 days. However, this reduction in the strength of the sample containing 30% slag at the age of 28 days is partially compensated so that this sample has 10% more compressive strength than the control sample, which may be due to the slow reaction of the slag. This process is intensified for concrete with 50% replacement of slag. The decrease in compressive strength can be attributed to the unavailability of free calcium hydroxide to create the pozzolanic reaction (Özbay et al., 2016).

For w/c = 0.28, the effects of various types of fibers, from long steel fibers (St), short steel fibers (SStl), PP, and HPP fibers as the combination was analyzed (Fig. 7). Using short steel fibers (SStl1.5), the compressive strength of this sample at 28 days is only 0.1% less than the strength of steel fibers with longer lengths. The 28-day compressive strength of the sample with 0.75% steel fibers (half the amount of steel fibers of the optimal sample) and 0.15% PP fibers is 8% less than the C0.28 + St1.5 sample. The compressive strength of the concrete is the highest for the C0.28-St1.5PP0.2 sample, which is about 5% less than the C0.28 + St1.5 sample. However, a comparison between the results of the sample breakage indicates that by combining the steel fibers and PP fibers, the concrete is more cohesive after breaking. Previous research showed that using a combination of steel fibers and PP, the properties of crack propagation improved, and its effect on the strength of the sample decreased (Deng et al., 2020; Ding et al., 2020).

Fig. 8 describes the compressive strength of concretes containing HPP. The 28-day compressive strength of HPP0.5 and HPP1 samples is much smaller than the C0.28 + St1.5 sample. In addition, by increasing HPP fibers, the compressive strength of concrete does not change significantly.

By adding 1% of steel fibers to samples with 0.5% of HPP fibers, the compressive strength of concrete increases. This increase is the impact of the steel fibers, and it may be concluded that HPP fibers do not increase compressive strength. However, the combination of PP fibers with HPP fibers does not perform well and has the lowest compressive strength of fiber concretes. Adding 1% of steel fibers to concrete which contains PP fibers and HPP fibers increased the compressive strength. In other words, in the range of fibers used in this research, long steel fibers significantly amplified the compressive strength of the samples.

The fracture appearance of the samples varies with various fibers. Comparing the failure of concrete with and without steel fibers, as indicated in Fig. 9a, b, the sample with fibers did not break after bearing the final load, and the concrete sample kept its overall shape and is relatively coherent. On the other hand, the control sample (without fiber) is entirely disintegrated, and the concrete sample does not disintegrate with the use of fiber, which can be considered a desirable feature. The mentioned trend can be observed in concrete containing steel fibers, PP fibers, and HPP fibers. In addition, among the silica fume and slag cement substitutes, the fracture of concrete containing silica fume is much more brittle than concrete containing slag. Griffith's theory suggests that brittle materials like concrete experience brittle fractures at low pressure due to the material's heterogeneous structure and the presence of numerous defects, such as microcracks and variously sized pores.

As the stress intensifies, the crack spreads quickly, with the number, length, and severity of the cracks continually growing. Stress concentration develops at the crack's tip and ultimately results in the crack propagating further. Crack development causes large cracks and destroys the structure of the material. Adding fibers to mixed concrete decreases the stress concentration caused by its heterogeneous distribution, leading to a more even distribution of stress within

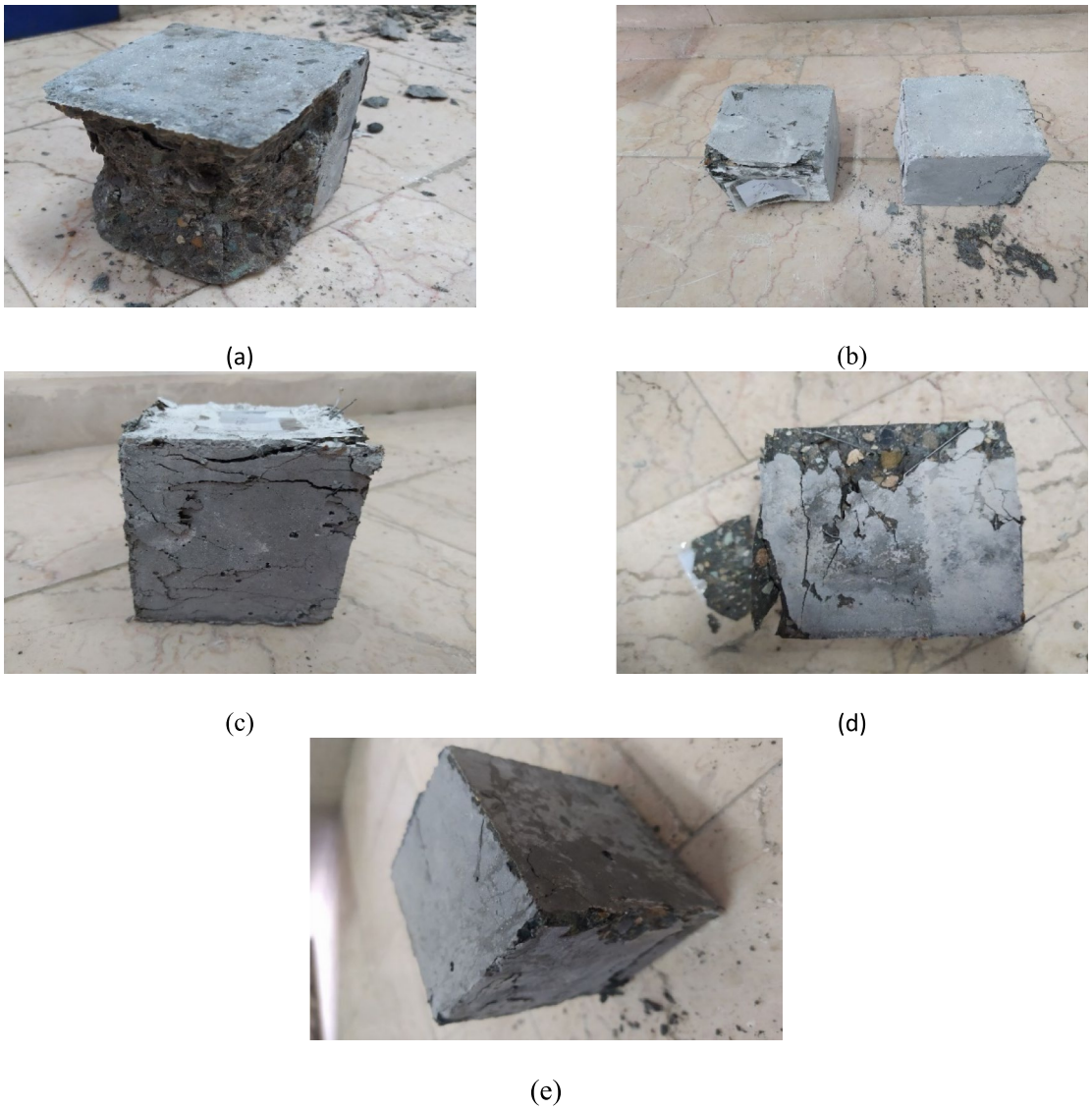

Fig. 9 Failure appearance of concrete in compressive strength test **a** without fiber; **b** with steel fiber; **c** with steel and polypropylene and HPP fiber; **d** contain silica fume; **e** contain slag

the material. The fibers inhibit crack formation and reduce the length of any cracks that do appear (Wu et al., 2019a).

The most important results of the compressive strength include the more significant effect of fibers on the compressive strength of early concrete ages (7 days), increasing the compressive strength of concrete by increasing the use of fibers up to 2%, the appropriate effect of fiber combination and replacing microsilica by 20%, the limited and even reducing effect of combining steel fibers and polypropylene fibers, and combining steel fibers with high-performance fibers.

3.2.2 Tensile Strength

Fig. 10 shows the tensile strength of the samples with w/c = 0.43, 0.38, 0.33, and 0.28, each containing steel fibers and subjected to standard curing. The tensile strength of the sample with steel fibers is approximately 20% greater than that of the control sample. For w/c = 0.38, the tensile strength of the sample containing fibers is 13% larger than that of the control sample. The tensile strength of the C0.33 + St1.5 sample is 47% greater than the C0.33 sample. For w/c = 0.28, incorporating 1.5% fibers boosted the tensile strength by approximately 31%. According to the results of this research, long steel fibers

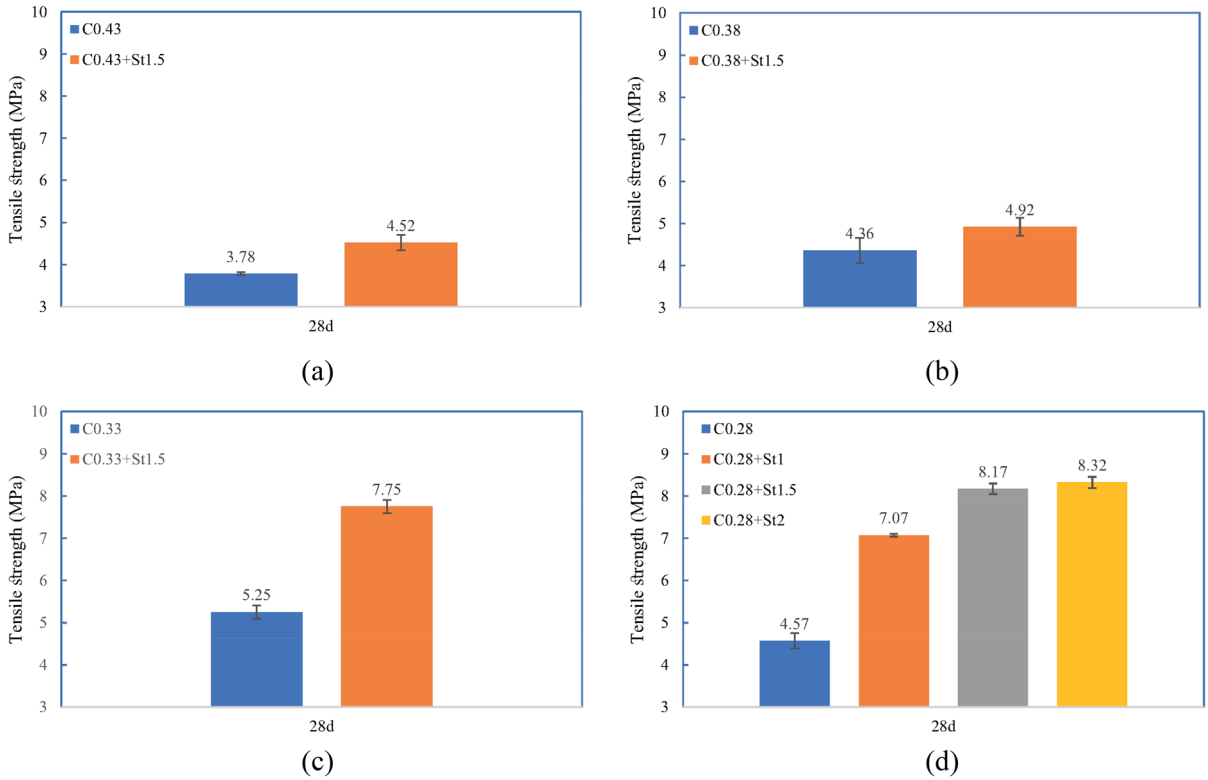

Fig. 10 Tensile strength in different w/c containing steel fibers at the age of 28 days; **a** w/c = 0.43; **b** w/c = 0.38; **c** w/c = 0.33; **d** w/c = 0.28

increase tensile strength notably. In general, the effect of increasing tensile strength is more significant in lower w/c values.

A comparison between the usage of different fiber percentages shows that by increasing the fiber volume, the tensile strength of concrete samples improves. The result is in line with previous research (Boulekbache et al., 2010b; Ibrahim et al., 2017; Richard & Cheyrezy, 1995; Wu et al., 2019b). For instance, the tensile strength of the C0.28 + St1 sample with 1% fibers was 30% more than the control sample. For a sample with 1.5% fibers, the tensile strength is 15% greater than that of the concrete sample with 1% fibers and 50% higher than that of the control sample. The sample with 2% steel fibers has only 1% more tensile strength than the sample with 1.5% fibers (Fig. 10d), which is not significant. Therefore, considering both economic factors and the impact on concrete workability, the C0.28 + St1.5 sample was chosen as the optimal one.

Fig. 11 indicates the tensile strength of concrete for w/c = 0.28 with 1.5% of steel fibers, silica fume cement substitutes, and iron furnace slag.

The tensile strengths of the concrete sample containing silica fume and the one with steel fibers but no silica fume were not significantly different. However, the more slag is used, the more tensile strength decreases. Hence, the tensile strength of the samples with 50% slag is 15% less than the sample with 30% slag and 44% less than the fiber sample (without cement substitute).

For w/c = 0.28, SStl and combinations of steel fibers with PP and HPP fibers were also used (Fig. 11b, c). The tensile strength of concrete using SStl is 21% smaller than the sample with long-length steel fibers. By reducing steel fibers and adding PP fibers, the tensile strength of the concrete sample decreased by about 30%. The best combination of steel fibers and PP in terms of tensile strength is C0.28 + St1.5 + PP0.2. In addition, in the use of HPP fibers, the optimal tensile strength using these fibers in concrete was not obtained, and using HPP1, a 40% decrease in tensile strength in comparison with the C0.28 + St1.5 sample occurred. The combination of these fibers with metal fibers leads to an increase of the tensile strength by 15% compared to HPP1 usage. Fig. 11 shows that the decrease in the w/c increased the tensile strength. For example, the tensile strength of the concrete sample with w/c = 0.28 is 4, 25, and 44%, more significant than the samples with w/c = 0.33, 0.38, and 0.43, respectively.

The results of the tensile strength test revealed an intriguing observation. During the splitting test, all

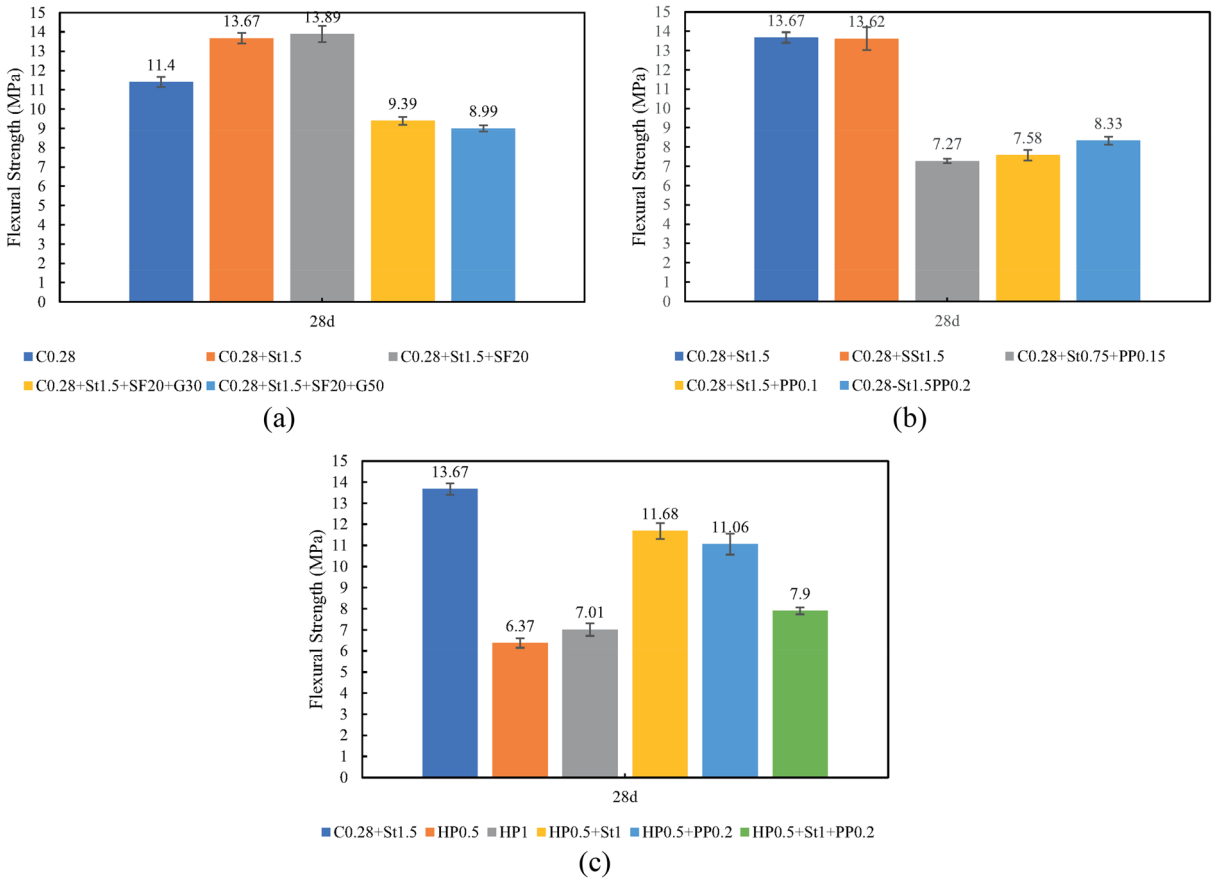

Fig. 11 Tensile strength for w/c = 0.28 at the age of 28 days; **a** containing long steel fibers, silica fume, and slag; **b** containing long, and short steel fibers, and polypropylene fibers; **c** contains long steel fibers, polypropylene, and high-performance polypropylene

cylindrical samples containing fibers remained unbroken, exhibiting only minor cracks (Fig. 12b). In contrast, the samples without fibers were completely fractured in half (Fig. 12a). In addition, Fig. 12c illustrates a sample reinforced with high-performance polypropylene fibers (HPP) and steel fibers.

The most effective type of fiber in tensile strength is steel fiber, and its optimal value is 1.5%, which has the most significant effect at a w/c = 0.33.

3.2.3 Flexural Strength

Fig. 13 indicates the flexural strength of the samples. Similar to the results of the compressive strength and tensile strength, the steel fibers increased the flexural strength of the samples.

The flexural strength of the C0.43 + St1.5 sample at w/c = 0.43 is about 3% higher than the C0.43 sample. In the w/c of 0.38, the flexural strength value is 12.42 MPa, which is 32% greater than the control sample. Eldin et al. (2014) stated that using steel fibers, the flexural strength increased even 40% more than that of samples without steel fibers. Eldin et al. (2014) incorporated up to 3% steel fiber in concrete with a w/c = 0.4, achieving a 40% increase in flexural strength at that dosage. In the present work, only 1.5% steel fiber was incorporated into the concrete, with a w/c = 0.38, resulting in a 32% increase in flexural strength compared to the control sample.

By decreasing w/c, the flexural strength also increases. The flexural strength of the C0.33 + St1.5 sample is 5% higher than the C0.38 + St1.5 sample. This sample has 30% more flexural strength than the control sample.

By increasing the percentage of fibers in the concrete samples, the flexural strength increased (Fig. 13d). The flexural strength of the C0.28 + St1.5 is 14% greater than the flexural strength of the C0.28 + St1 sample. According to research (Abbas et al., 2015; Yu et al., 2014a), the flexural strength after cracking, three-point bending strength parameters, and fracture energy increase almost linearly with the fiber volume increase. The flexural strength of the C0.28 + St2 sample with 2% fibers is 4% higher than C0.28 + St1.5 concrete.

Fig. 12 Failure appearance of concrete samples in tensile strength test **a** without fiber; **b** with steel fiber; **c** with steel and HPP fiber

Fig. 14a presents the result of the samples, where part of the cement is substituted with silica fume powder and slag. By replacing silica fume, the flexural strength increased by 1%, but by replacing slag in fiber concrete, the flexural strength decreased by 32 and 35%, respectively, at 30 and 50% replacement with slag.

Fig. 14b shows the effect of fiber types on the flexural strength of samples. A comparison of concrete containing short and long steel fibers indicates the flexural strength of short steel fibers in concrete samples is almost equal to that of long steel fibers. However, the addition of 0.15% of PP fibers to the concrete samples with steel fibers (to the amount of 0.75%) reduced the flexural strength of the samples by 47%. Despite the samples containing a high proportion of steel fibers (1.5%) combined with PP, their flexural strength decreased by 40–45%.

One of the important reasons for these results is that the purpose of using PP fibers is not to enhance the mechanical properties of concrete samples, and one of the most important reasons for its use is to prevent microcracks caused by shrinkage. In addition, among other causes, it can be stated that the bond quality between cement matrix and PP fibers is poor (Lv et al., 2021).

In concrete with HPP fibers in combination with PP and steel fibers (Fig. 14c), the flexural strength of concrete with HPP0.5 and HPP1 samples is 54 and 51% less than the control fiber concrete (C0.28 + St1.5 sample). By adding 1% of steel fibers along with these fibers, the flexural strength increased by 66%, and by adding PP fibers along with HPP fibers, the flexural strength decreased by 6% compared to the case with steel fibers. However, using all three types of fibers,

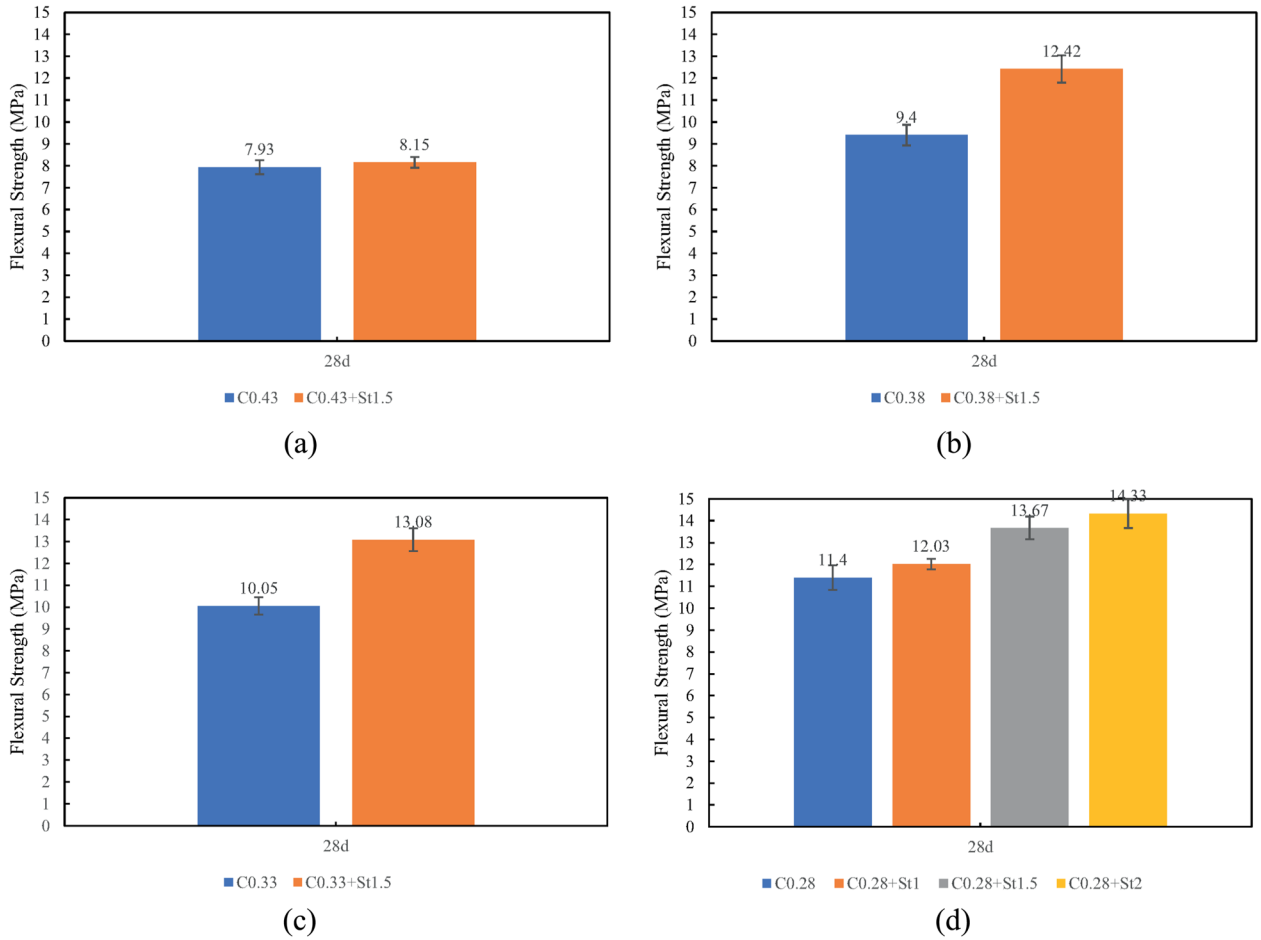

Fig. 13 Flexural strength in different w/c containing steel fibers at the age of 28 days; **a** w/c = 0.43; **b** w/c = 0.38; **c** w/c = 0.33; **d** w/c = 0.28

a flexural strength decreased by 29 and 33% compared to the concrete samples using HPP0.5 + St1 and HPP0.5 + PP0.2, respectively. The flexural strength of concrete with fiber composition is less than that of concrete reinforced with steel fibers.

The form of breaking the flexural samples is similar to the other two tests of compressive strength and tensile strength (bisection) so that the sample without fibers is split in half after reaching the breaking force threshold and the whole sample is broken (Fig. 15). However, concrete with steel fibers only cracks after bearing the final load. It can maintain its structure, and the sample is not divided into two halves.

The behavior of concrete with fibers in the three-point flexural strength is very similar to the tensile strength. However, the weakening effect of non-steel fibers in flexural strength is more significant.

3.3 Thermal Curing Effects on HPC

3.3.1 Compressive Strength

Table 6 presents the compressive strength of 7 and 28 days of concrete in different w/c in thermal and standard curing. For w/c = 0.43, in the comparison of two standard and thermal curing, at the age of 7 days, the compressive strength of CH0.43 is 18% less than the sample curing under standard conditions (C0.43). Even the thermal curing made fiber concrete, CH0.43 + St1.5 sample, reached 37% lower compressive strength than C0.43 concrete.

Fig. 16 indicates the compressive strength of samples in different w/c containing steel fibers in standard and thermal curing at the ages of 7 and 28 days. At 7 days, the compressive strength of the C0.43 + St1.5 is 10% greater than the thermally cured specimen. At the w/c of 0.38 at 7 days, the compressive strength of the CH0.38 is 42% greater than the compressive strength of the C0.38

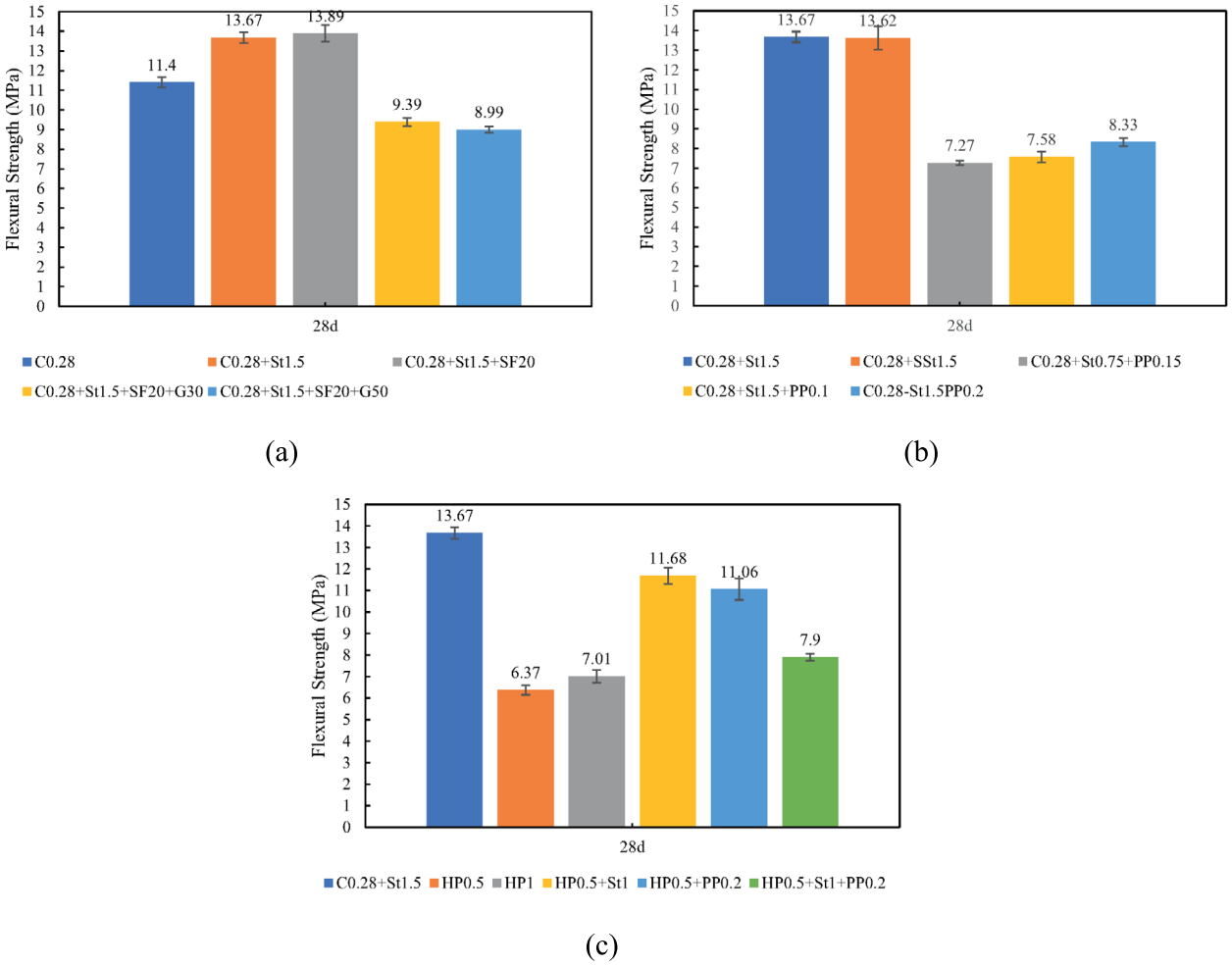

Fig. 14 Flexural strength in w/c = 0.28 at the age of 28 days; **a** containing long steel fibers, micro-silica, and slag; **b** containing long, short, and polypropylene steel fibers; **c** contains long steel fibers, polypropylene, and high-performance polypropylene

Fig. 15 Failure appearance of concrete samples in flexural strength test **a** without fiber; **b** with steel fiber

sample and 9% higher than the CH0.38 + St1.5 sample. The C0.38 + St1.5 concrete sample has 10% more compressive strength than the CH0.38 + St1.5 sample.

For w/c = 0.33, the decrease in the compressive strength of the thermally cured sample in comparison with the standard sample at the age of 7 days in concrete without

Table 6 Compressive strength of samples in different w/c containing steel fibers in standard and thermal curing at the ages of 7 and 28 days

Concrete type	Curing	Concrete code	Compressive strength		
			7 days	28 days	90 days
Without fiber	Thermal	CH0.43	26.7	32.1	–
		CH0.38	54	56.6	–
		CH0.33	38.4	43.5	–
	Standard	C0.43	32.3	46.5	60.56
		C0.38	38.9	51.5	61.83
		C0.33	57.9	63.3	70.16
With steel fiber	Thermal	CH0.43 + St1.5	41.8	51.6	–
		CH0.38 + St1.5	49.2	61.5	–
		CH0.33 + St1.5	52.4	56.8	–
	Standard	C0.43 + St1.5	46.1	53.50	61.2
		C0.38 + St1.5	54.3	65.66	67.6
		C0.33 + St1.5	63.0	68.60	70.5

fibers is 34%, and in fiber concrete (CH0.38 + St1.5) is 27%.

In this study, it was found that thermal curing (without steam) generally disrupts the achievement of compressive strength in concrete. This effect occurs in both fiber-reinforced and non-fiber-reinforced concrete. However, incorporating steel fibers into the concrete mitigated the adverse impact of thermal curing on compressive strength.

3.3.2 Tensile Strength

Fig. 17 indicates the tensile strength of thermal and standard curing concrete samples at the age of 28 days. The heat treatment decreased the tensile strength of the sample. For w/c = 0.43, thermal curing reduced the tensile strength of concrete by 37%. In this ratio of water to cement and with the use of fibers, the tensile strength of concrete decreased by 65% due to thermal curing, which can point out the negative effect of thermal without moisture on concrete.

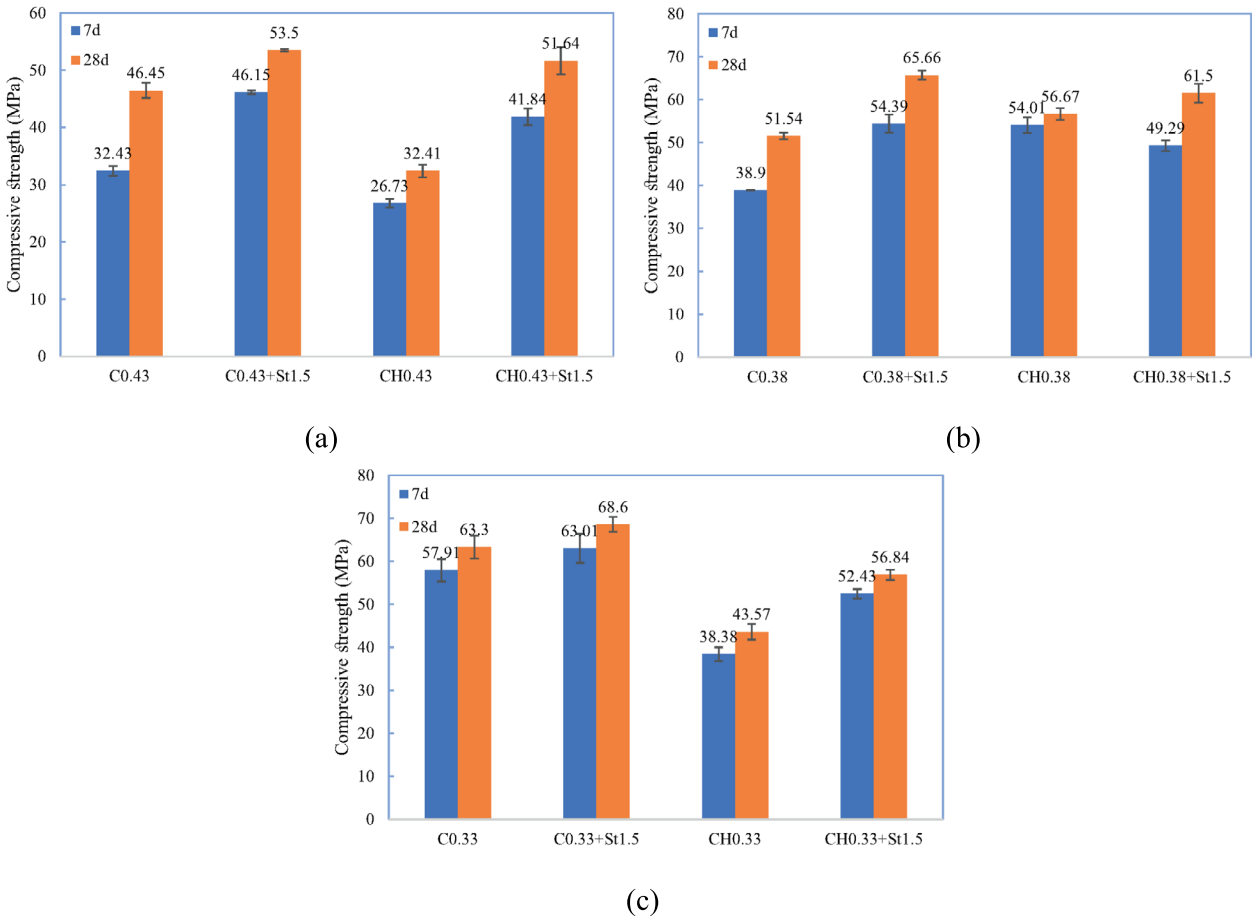

Fig. 16 Compressive strength in different curing conditions [standard (C) and thermal (CH)], **a** C0.43, CH0.43; **b** C0.38, CH0.38; **c** C0.33, CH0.33

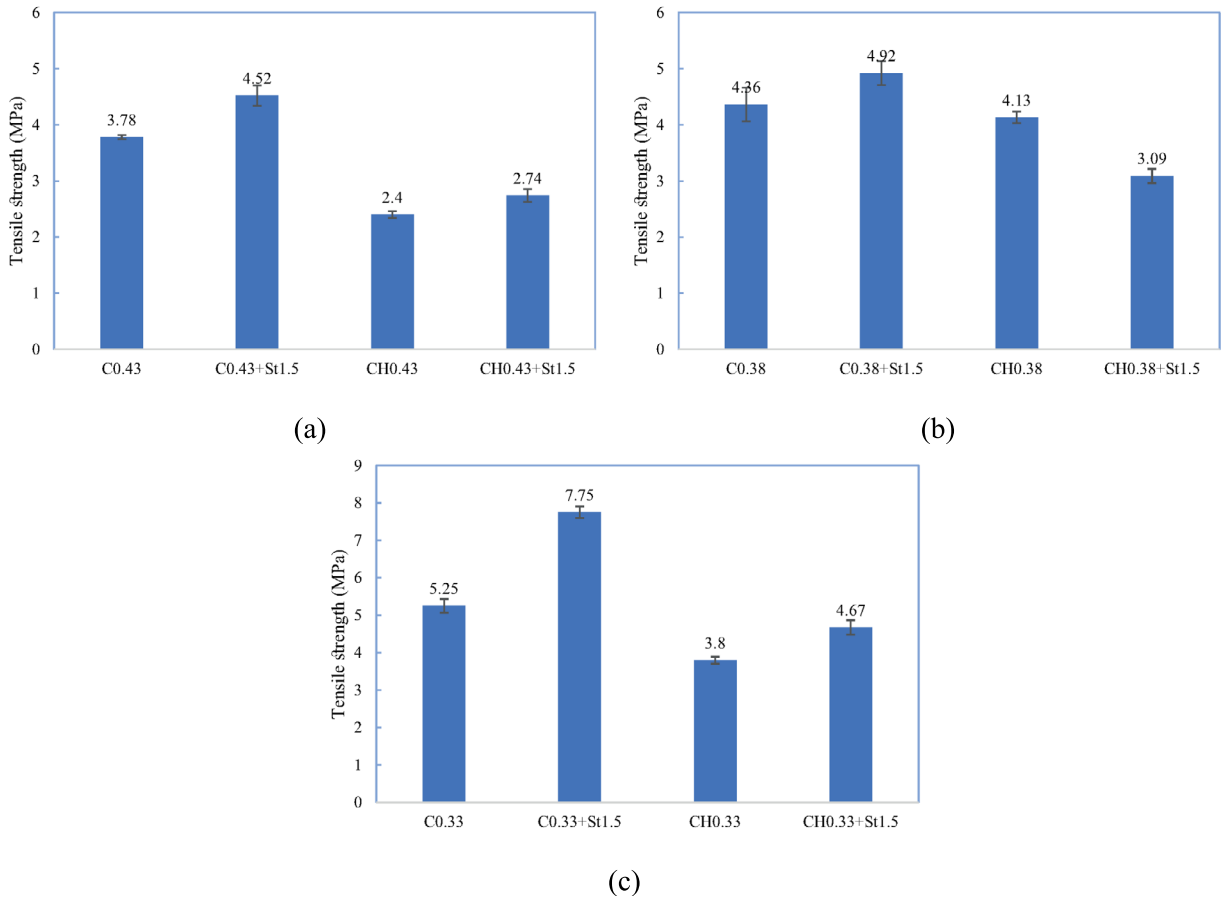

Fig. 17 Tensile strength in different curing conditions [standard (C) and thermal (CH)], **a** C0.43, CH0.43; **b** C0.38, CH0.38; **c** C0.33, CH0.33

In the w/c of 0.38, the tensile strength of the CH0.38 sample decreased by 60% compared to C0.38 + St1.5. It is clear that using the St fiber, the tensile strength of the samples increased by about 33% and 13% in C0.38 + St1.5 and CH0.38 + St1.5 compared to the C0.38 and CH0.38 samples, respectively. The thermal curing decreased the tensile strength of the samples. For example, the tensile strength of the CH0.38 and CH0.38 + St1.5 decreased by 41% and 19% compared to C0.38 and C0.38 + St1.5, respectively.

In the w/c of 0.33, the C0.33 + St1.5 sample also has 40% more tensile strength than the CH0.33 + St1.5 sample, and the sample without heat-cured fibers has a 28% reduction in tensile strength from its standard condition. According to the results of this research, heat curing has had an adverse effect on tensile strength, which is more unfavorable in tensile strength than in compressive strength.

3.3.3 Flexural Strength

Fig. 18 presents the flexural strength of the cured samples in thermal and standard conditions. Thermal curing without steam decreases the flexural strength of concrete. The flexural strength of the C0.43 + St1.5 sample is 15% higher than CH0.43 + St1.5. For identical w/c, the sample without fiber with thermal curing has 35% less flexural strength than the sample cured in standard conditions.

For w/c = 0.38, the flexural strength of the CH0.38 is 43% smaller than the C0.38. In addition, the CH0.38 + St1.5 sample had a 29% reduction of flexural strength in comparison with the C0.38 + St1.5 sample. In the w/c of 0.33, the flexural strength of the C0.33 + St1.5 sample is 30% higher than the CH0.33 + St1.5 sample. The flexural strength of the CH0.33 sample is smaller than that of the C0.33 and CH0.33 + St1.5 samples by 41 and 40%, respectively. Thermal curing without steam contains a destructive impact on the flexural strength of concretes in different w/c. This negative effect persists with the addition of steel fibers, although it is reduced.

3.4 Effect of Sulfate Environment on HPC

For modeling the concrete exposure to a sulfate environment, which can be due to contact with water containing sulfate ions or wet soils containing this ion, cubic samples

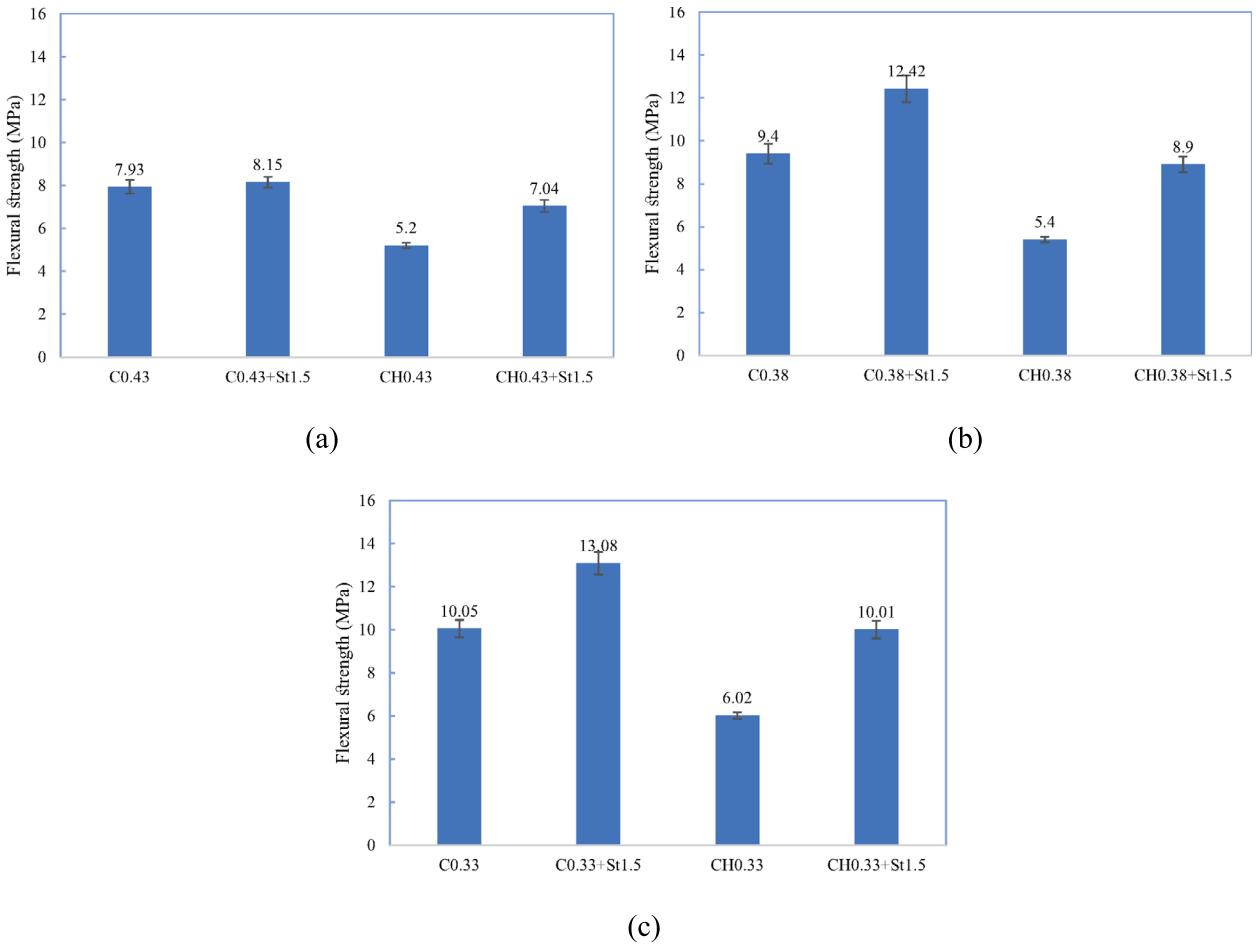

Fig. 18 Flexural strength of concretes in different curing conditions [standard (C) and thermal (CH)], **a** C0.43, CH0.43; **b** C0.38, CH0.38; **c** C0.33, CH0.33

(10 cm) after 28 days of standard curing, up to 365 days were immersed in sulfate solution with a concentration of 5% (Fig. 19).

Due to the limitations of the experiments, only the compressive strength test was carried out on the samples. The 365-day compressive strength value in the sulfate environment was compared with the 90-day concrete compressive strength results in standard conditions. For w/c = 0.43, the compressive strength of the fiber-free concrete specimen (C0.43) after 1 year of curing in a sulfated environment has a 58% drop in compressive strength as compared to the 90-day standard concrete.

Using steel fibers in concrete with w/c = 0.43 reduced the decrease in compressive strength to just 15%. For w/c = 0.43, the compressive strength of the sample without fibers after 1 year in sulfate curing was decreased by almost 16%, and using the steel fibers, this reduction reached 7% (Fig. 20).

The impact of reducing the sulfate curing on compressive strength using steel fibers for w/c = 0.33 and 0.28 can also be observed. In the w/c of 0.33, the use of fibers caused a decrease in compressive strength from about 19% to approximately 7%. In the w/c of 0.28, the compressive strength reduction decreased from 14 to 10%.

Therefore, in concretes with different w/c, the use of fibers meaningfully limits the damage caused by the sulfate environment in samples. The amount of damage is more significant in high w/c. It also shows how the concrete breaks the application of fibers, making the overall structure of the concrete remain somewhat in the form of the original cube after the break (Fig. 17).

At w/c = 0.28, the study explored the effects of fiber application, cement substitutes, and different types of fibers. In concrete with w/c = 0.28, after 365 days, a 14% drop in compressive strength occurred, which reached 10% with the use of 1.5% fibers. One of the key reasons for the reduced destructive effects in concrete containing steel fibers is that the fibers delay the initiation and propagation of microcracks. This mechanism minimizes damage and failure in concrete during freezing and thawing

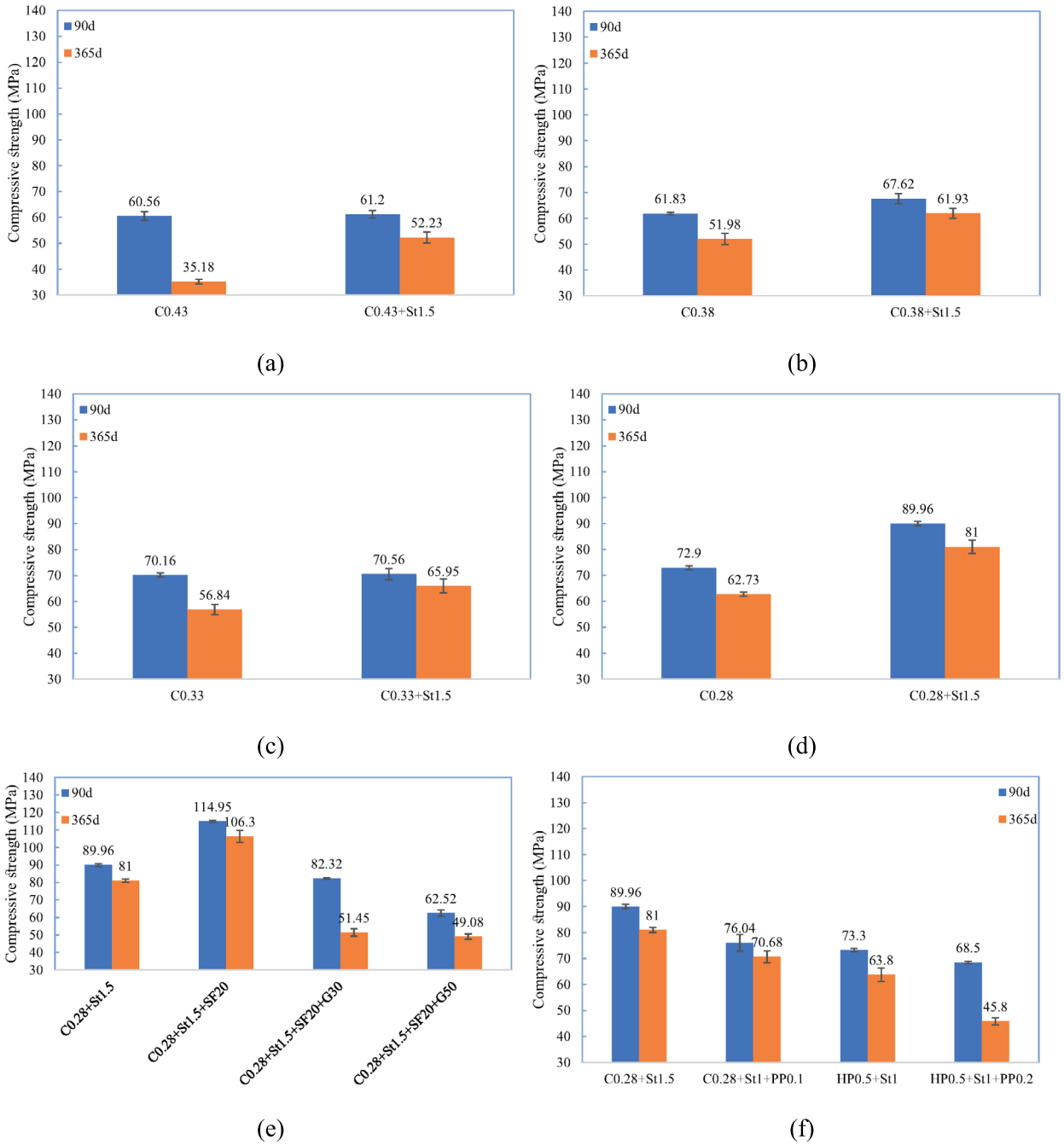

Fig. 19 Compressive strength of concretes with and without fibers at 90 days (standard curing) and 365 days (curing in sulfate environment); **a** w/c = 0.43; **b** w/c = 0.38; **c** w/c = 0.33; **d** w/c = 0.28 with steel fibers; **e** w/c = 0.28 with fiber and cement substitute; **f** w/c = 0.28 with all kinds of fibers

cycles as well as under sulfate attack conditions. Moreover, the enhancement of fiber-reinforced concrete's failure mechanism correlates with its capacity to bridge and restrain the cracking of steel fibers (Abbas et al., 2015).

For identical w/c value and comparing the samples with silica fume and slag, the C0.28 + St1.5 + SF20 sample has only a 7% loss of compressive strength and has the best performance against sulfate attack. When silica fume substitutes cement, it reacts chemically with cement hydration products to form calcium silicate hydrates, thus inhibiting the formation of gypsum and

Fig. 20 Appearance of concrete with steel fiber in compressive strength **a** before testing; **b** after testing

ettringite by halting the reaction of sulfate salts with cement hydration products.

Moreover, as the pozzolanic effect of the substitution materials increases, the production of cement gel is enhanced. Consequently, the formation of weak materials due to sulfate attack is minimized, and the porosity of the concrete is reduced (C. et al., 2002). However, concrete with 30 and 50% slag has a reduction in strength of 37.5 and 21.5%, respectively. In the examination of the samples with mixed fibers, the reduction of concrete compressive strength in sulfate conditions in C0.28 + St1 + PP0.1, HP0.5 + St1, and HP0.5 + St1 + PP0.2 concretes is 8, 13, and 24%, respectively.

3.5 Microstructure

The difference in mechanical properties and durability of concretes can be described by evaluating their microstructure. In this research, SEM imaging (Fig. 21) was employed to analyze the microstructure of concrete. The study examined the microstructure and morphology of three types of concrete samples: (1) the C0.28 concrete sample, used as the reference (control) sample; (2) the C0.28 + St1.5 + SF20 sample, containing steel fibers and silica fume; and (3) the C0.28 + St1.5 + SF20 + G30 sample, incorporating steel fibers, silica fume, and slag.

The image of concrete sample C0.28 indicates that the cement paste has good uniformity, and it is evident that the calcium silicate hydrates gel is extensively distributed in the high-performance concrete (HPC) paste structure (Fig. 21a). The SEM image indicates that the hardened paste structure is dense. This is because of the low w/c and cement hydration, and most calcium silicate hydrate products are uniform. In addition, this figure shows that for w/c = 0.28, the interfacial transition zone (ITZ) between the aggregates and the paste matrix exhibits low porosity and few pores.

Fig. 21b indicates the SEM of concrete with silica fume (C0.28 + St1.5 + SF20 sample). The presence of silica fumes in the sample increases the calcium silicate hydrate gel and decreases C–H. Silica fume reacts with calcium hydroxide ($Ca(OH)_2$) to generate extra calcium silicate hydrates gel. In addition, owing to the pozzolanic reaction of silica fume, the cement paste is denser and more uniform. The ITZ region in this concrete sample also looks like a dense matrix.

In C0.28 + St1.5 + SF20 + G30 concrete sample, where 30% of slag is also replaced by cement (Fig. 21c), C–S–H gel has less cohesion and uniformity than C0.28 and C0.28 + St1.5 + SF20 concretes. Slag mainly acts as filler material (Georget et al., 2021; Gupta, 2014; Tahwia et al., 2021).

Also, through the EDX test, the compositions of C0.28, C0.28 + St1.5 + SF20, and 0.28 + St1.5 + SF20 + G30 samples were determined through spectroscopic analysis (Fig. 22). When 20% of cement is substituted with silica fume, a rise in micro-silica content is observed as compared to the control sample. The attendance of silica fume in the mixture increased the silica and led to the generation of calcium silicate hydrates gel, which is the key product of the pozzolanic reaction. Therefore, the mechanical characteristics and durability of these samples are enhanced by filling the internal voids with C–S–H gel.

In the case of mixtures containing 30% substitution of cement with slag, the silica content is reduced compared to the other two samples. The main product of hydration in samples with silica fume is calcium silicate hydrates, and the Si/Ca are significantly increased in comparison with the control concrete. In addition, Ca/Si decreases, which indicates increasing compressive strength of the concrete specimen.

Fig. 23 illustrates that Ettringites were absent in all the analyzed concrete samples. A lot of C–S–A–H gel was observed in the control sample, which was not present in the other two samples. The amount of nano-silica that contributes to the structure and strength of concrete in the other two samples is much higher than in the control sample. In fact, using cement substitutes such as micro-silica, the amount of nano-silica increases. In addition, the C0.28 + St1.5 + SF20

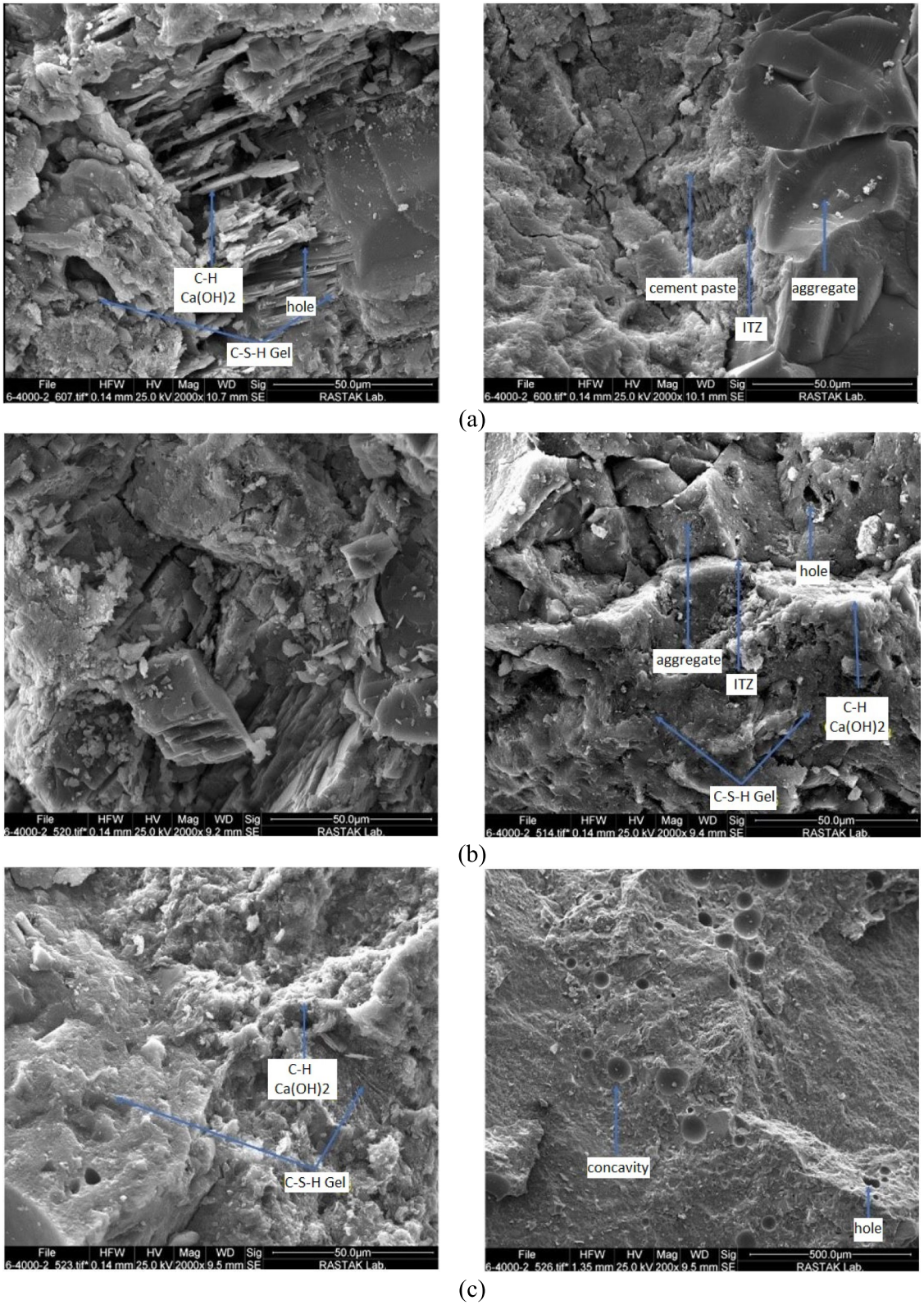

Fig. 21 Analysis of the scanning electron microscope (SEM) images of the samples at the age of 28 days; **a** C0.28; **b** C0.28 + St1.5 + SF20; **c** C0.28 + St1.5 + SF20 + G30

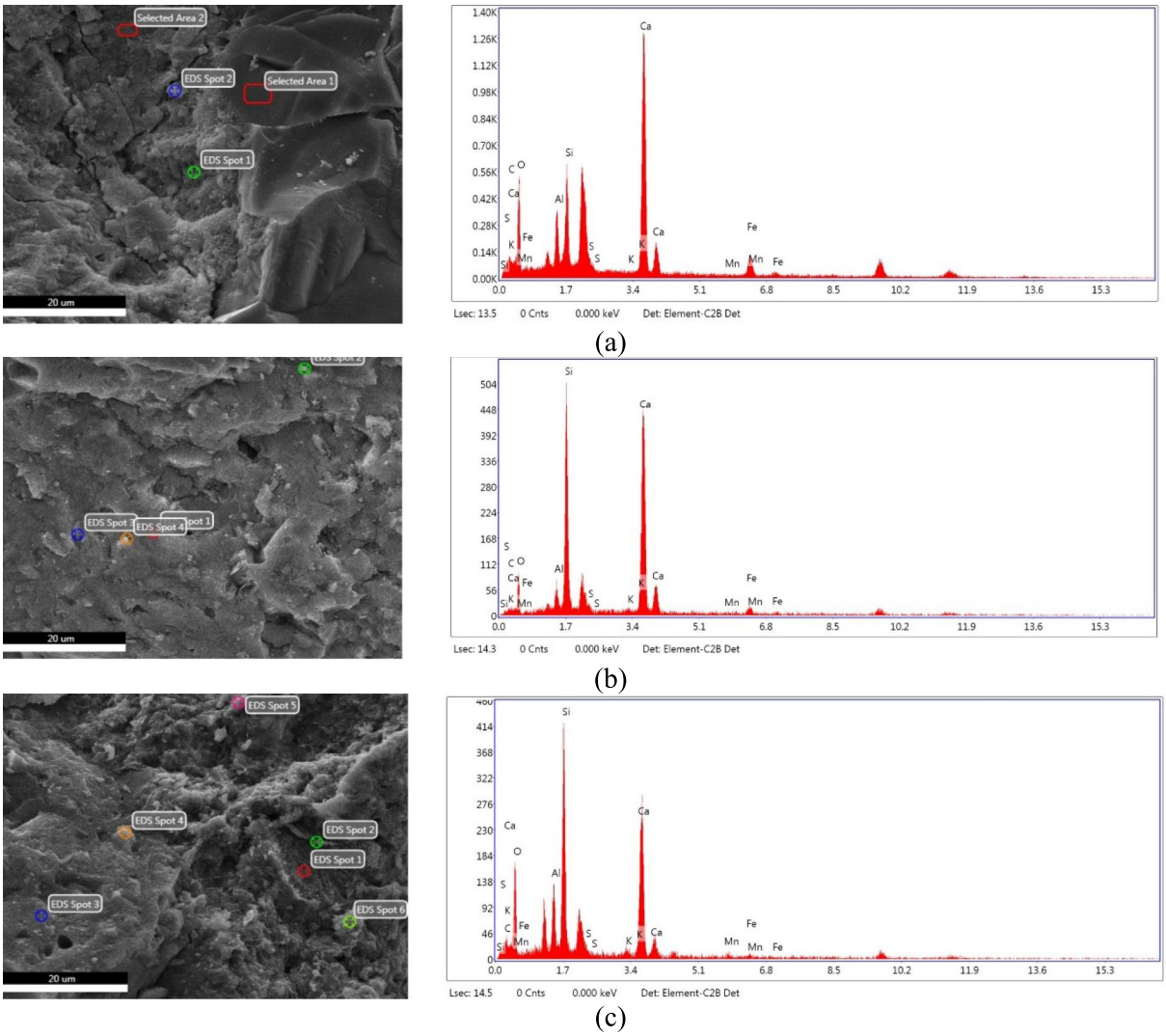

Fig. 22 EDX test results of samples at the age of 28 days; **a** C0.28; **b** C0.28 + St1.5 + SF20; **c** C0.28 + St1.5 + SF20 + G30

sample has more nano-silica compared to the other two samples.

4 Conclusions

In this study, the characteristics of concrete, including workability, mechanical, and durability, were investigated experimentally. The experiments were conducted for different fibers and water-to-cement ratios in standard, thermal, and sulfate environmental curing. The results are summed up as follows:

1. Using the fibers in the concrete samples, the workability of the concrete decreases. This reduction is more apparent in mixtures of mixed fibers with steel fibers, especially polypropylene fibers.
2. The use of steel fibers in concrete improves mechanical characteristics and durability. Therefore, for water-to-cement equal to 0.28, the application of 1.5% of metal fibers enhanced the compressive strength by 25%, tensile strength by 50%, and flexural strength by 20% at 28 days in comparison with the sample without fibers. By increasing the percentage of steel fibers in a concrete sample, the mechanical properties such as compressive, tensile, and flexural strengths also rise. The difference in strength between using 2 and 1.5% steel fibers is negligible.
3. Among all samples, a sample that contains 20% silica fume has the highest compressive strength. On the other hand, the 28-day compressive strength of this sample is 25% higher than the sample without microsilica. Likewise, the tensile and flexural strength of this sample is greater than that of other samples, but

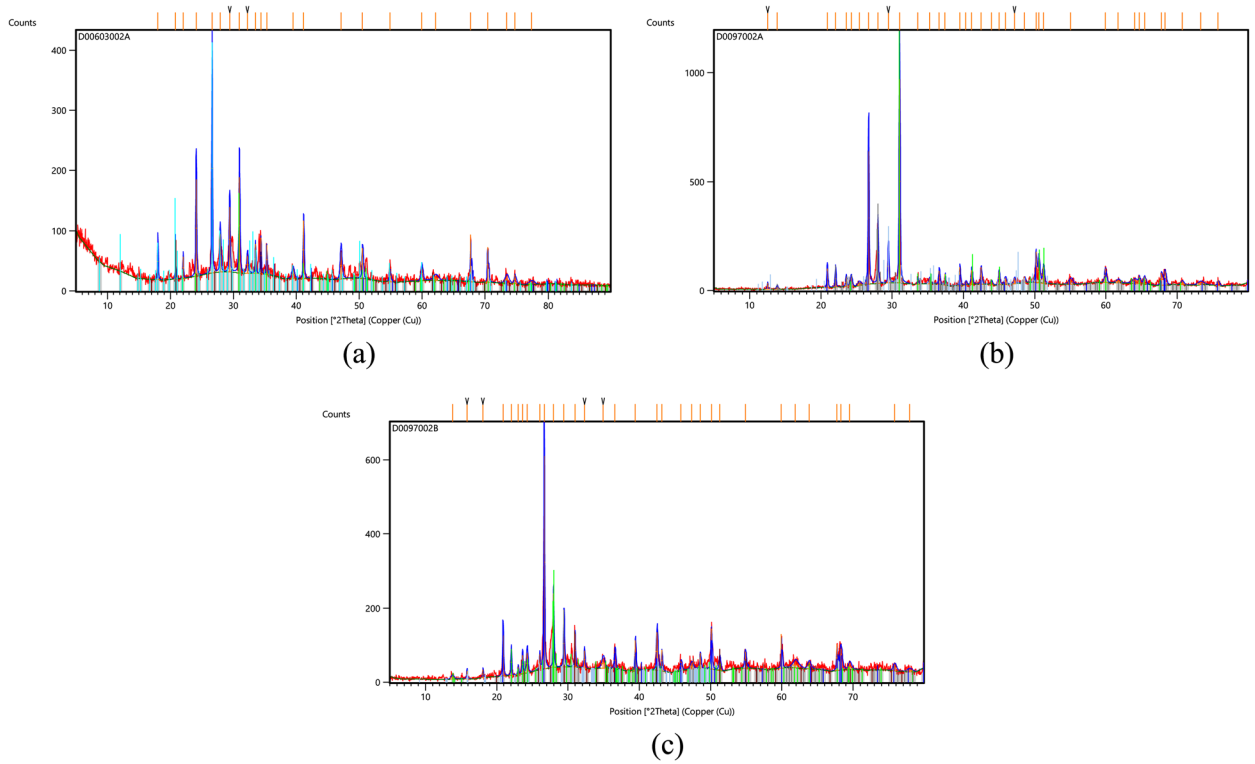

Fig. 23 XRD results of concrete samples at the age of 28 days; **a** C0.28; **b** C0.28 + St1.5 + SF20; **c** C0.28 + St1.5 + SF20 + G30

the change in strength is minimal in comparison with the compressive strength. However, using blast furnace slag in samples, the compressive, tensile, and flexural strength of the samples decreased, which increases with the increase in the amount of slag. One of the reasons for this decrease in resistance can be due to the low quality of slag used in this study.

4. Using combined fibers, including steel, PP, and HPP fibers, the best compressive strength occurred for the samples with 1% steel fibers and 0.2% PP fibers. The compressive strength of this concrete is 81.73 MPa. It is 5% smaller than the sample with 1.5% steel fibers. In addition, among the samples with different fibers, the sample with 1% steel fibers, 0.5% HPP fibers, and 0.2% PP fibers has the best tensile strength (7.53 MPa). The flexural strength of the sample with 1% steel fibers and 0.5% HPP fibers has the highest flexural strength (11.68 MPa) among concretes with mixed fibers.
5. The amount of steel fibers was tested in three amounts: 1, 1.5, and 2%. Results showed that the amount of 1.5% is the optimal amount of use, because the amount higher than 1.5% of steel fibers, the concrete mixture is faced with a more significant decrease in workability, and molding, compaction and surface finishing was more difficult
6. Curing concrete at high temperatures without sufficient moisture (steam), even with a temperature range with appropriate growth and temperature drop at a maximum temperature of 70 °C, causes weakness in the mechanical characteristics of the concrete, such as compressive strength, tensile strength, and bending strength. Using steel fibers in concrete does not prevent the damage caused in concrete.
7. Placing concrete in a sulfated environment causes weakness in concrete and decreases its mechanical properties. In the concretes that were exposed to sodium sulfate solution after 28 days of standard curing up to 365 days, the compressive strength of the concrete decreased as the water-to-cement ratio decreased. Using steel fibers in concrete limited the compressive strength reduction. Using the silica fume caused the concrete to obtain the least loss in the sulfate environment.
8. According to SEM images and XRD results, the sample with micro-silica has a denser structure and more C–S–H gel than other samples. In addition, the sample containing slag has fewer pores than the other two samples, which is due to the filling property of the slag.

The data of this study improve the knowledge of the effects of the fibers on the workability and mechanical characteristics of concrete containing different types of fibers, as well as cement substitutes of concrete under standard, thermal, and sulfate environment curing conditions. For future research, the force–displacement curve of the flexural test and the stress–strain curve of the compression test can be analyzed. These data provide critical insights (such as ductility, post-failure behavior, etc.) that may be used for structural design.

Acknowledgements
We are very grateful to all the staff of the concrete laboratory of Karazmi University.

Author contributions
Shiva Safari Taleghani conducted experiments and drafted manuscript. Amir Masoud Salehi analyzed data and drafted the manuscript. Mojtaba Mehraein wrote the draft manuscript. Gholamreza Asadollahfardi assisted in revising the manuscript.

Funding
This research received no specific grant from any funding agency in the public, commercial, or not-for-profit sectors.

Data Availability
The data sets used and/or analyzed during the current study are available from the corresponding author on reasonable request.

Declarations

Competing Interests
The authors declare that they have no competing interests.

Received: 12 July 2024 Accepted: 30 June 2025
Published online: 08 September 2025

References

Abbas, S., Soliman, A. M., & Nehdi, M. L. (2015). Exploring mechanical and durability properties of ultra-high performance concrete incorporating various steel fiber lengths and dosages. *Construction and Building Materials, 75*, 429–441. https://doi.org/10.1016/j.conbuildmat.2014.11.017

Abdi Moghadam, M., & Izadifard, R. A. (2021). Prediction of the tensile strength of normal and steel fiber reinforced concrete exposed to high temperatures. *The International Journal of Concrete Structures and Materials, 15*, 47.

Afroughsabet, V., Biolzi, L., & Ozbakkaloglu, T. (2016). High-performance fiber-reinforced concrete: a review. *The Journal of Materials Science, 51*, 6517–6551. https://doi.org/10.1007/s10853-016-9917-4

Afroughsabet, V., & Teng, S. (2020). Experiments on drying shrinkage and creep of high-performance hybrid-fiber-reinforced concrete. *Cement and Concrete Composites, 106*, Article 103481. https://doi.org/10.1016/j.cemconcomp.2019.103481

Aiamsri, K., Yaowarat, T., Horpibulsuk, S., Suddeepong, A., Buritatum, A., Hiranwatthana, K., & Nitichote, K. (2024). Bonding behavior of lap-spliced reinforcing bars embedded in ultra-high-performance concrete with steel fibers. *Developments in the Built Environment, 20*, Article 100585. https://doi.org/10.1016/j.dibe.2024.100585

Antarvedi, B., & Banjara, N. K. (2023). S, Singh Optimization of polypropylene and steel fibers for the enhancement of mechanical properties of fiber-reinforced concrete. *Asian Journal of Civil Engineering, 24*, 1055–1075.

ASTM C136-84a. (1984). Standard Test Method for Sieve Analysis of Fine and Coarse Aggregates, ASTM International, West Conshohocken, PA.

ASTM C1240. (2003). Standard specification for silica fume used in cementitious mixtures. West Conshohocken, PA, USA: ASTM International.

ASTM C 1012. 2004. Test method for length change of hydraulic-cement mortars exposed to a sulfate solution. Annual book of ASTM Standards, Vol. 04.01.

ASTM E1621-13. (2013). Standard guide for elemental analysis by wavelength dispersive x-ray fluorescence spectrometry, West Conshohocken, PA.

ASTMC496/C496M. (2017). Standard Test Method for Splitting Tensile Strength of Cylindrical Concrete Specimens,. ASTM International (ASTM).

ASTM C150/C150M-18. (2018). Standard specification for portland cement, ASTM International, West Conshohocken, PA.

ASTM C1609/C1609M-19a. (2019). Standard Test Method for Flexural Performance of Fiber-Reinforced Concrete (Using Beam with Third-Point Loading), ASTM International, West Conshohocken, PA.

ASTM C192. (2019). Standard Practice for Making and Curing Concrete Test Specimens in the Laboratory in, ASTM International, West Conshohocken, PA.

ASTM C143/C143M-20. (2020). Standard Test Method for Slump of Hydraulic-Cement Concrete, ASTM International, West Conshohocken, PA.

Boulekbache, B., Hamrat, M., Chemrouk, M., & Amziane, S. (2010a). Flowability of fiber-reinforced concrete and its effect on the mechanical properties of the material. *Construction and Building Materials, 24*, 1664–1671. https://doi.org/10.1016/j.conbuildmat.2010.02.025

Boulekbache, B., Hamrat, M., Chemrouk, M., & Amziane, S. (2010b). Flowability of fibre-reinforced concrete and its effect on the mechanical properties of the material. *Construction and Building Materials, 24*, 1664–1671. https://doi.org/10.1016/j.conbuildmat.2010.02.025

BSEN123903. (2019). Testing hardened concrete Part 3: Compressive strength of test specimens. British Standards Institution (BSI), pp. 12390–3.

C-16 A. Standard Guide for Examination of Hardened Concrete Using Scanning Electron Microscopy. 2016. [(accessed on 26 November 2021)]. Available online: https://standards.globalspec.com/std/3862671/ASTM%20C1723-16.

Chan, Y. W., & Chu, S. H. (2004). Effect of silica fume on steel fiber bond characteristics in reactive powder concrete. *Cement and Concrete Research, 34*, 1167–1172. https://doi.org/10.1016/j.cemconres.2003.12.023

Chen, M., Feng, J., Cao, Y., & Zhang, T. (2023). Synergetic effects of hybrid steel and recycled tire polymer fibers on workability, mechanical strengths and toughness of concrete. *Construction and Building Materials, 368*, 13042. https://doi.org/10.1016/j.conbuildmat.2023.130421

Deng, F., Xu, L., Chi, Y., Wu, F., & Chen, Q. (2020). Effect of steel-polypropylene hybrid fiber and coarse aggregate inclusion on the stress–strain behavior of ultra-high performance concrete under uniaxial compression. *Composite Structures, 252*, Article 112685. https://doi.org/10.1016/j.compstruct.2020.112685

Ding, Y. Q., Wang, F., Pacheco-Torgal, F., & Yulin, Z. (2020). Hybrid effect of basalt fiber textile and macro polypropylene fiber on flexural load-bearing capacity and toughness of two-way concrete slabs. *Construction and Building Materials, 261*, Article 119881. https://doi.org/10.1016/j.conbuildmat.2020.119881

Edgington, J., Hannant, D. J., Williams, R. I. T. (1974). Steel Fibre Reinforced Concrete, Fibre Reinforced Materials. The Construction Press, Lancaster. England. pp. 112–128.

Eldin, H. K. S., Mohamed, H. A., Khater, M., & Sayed, S. A. (2014). Mechanical properties of ultra-high performance fiber reinforced concrete. *International Journal of Engineering and Technology Innovation (IJETI), 4*, 4–10.

Georget, F., Wilson, W., & Scrivener, K. L. (2021). edxia: Microstructure characterization from quantified SEM-EDS hypermaps. *Cement and Concrete Research*. https://doi.org/10.1016/j.cemconres.2020.106327

Gu, C., Sun, W., Guo, L., & Wang, Q. (2016). Effect of curing conditions on the durability of ultra-high performance concrete under flexural load. *Journal of Wuhan University of Technology-Mater. Sci. Ed., 31*, 278–285.

Gupta, S. (2014). Development of ultra-high performance concrete incorporating blend of slag and silica fume as cement replacement. *International Journal of Civil and Structural Engineering Research (IJCSER), 2*, 35–51.

Hadeed, M., Humid, A. M., & Al-Gburi, M. (2023). Utilization of hybrid fibers in different types of concrete and their activity. *The Journal of the Mechanical Behavior of Biomedical Materials., 368*, Article 130421. https://doi.org/10.1515/jmbm-2022-0262.Mater

Helmi, M., Hall, M. R., Stevens, L. A., & Rigby, S. P. (2016). Effects of high-pressure/temperature curing on reactive powder concrete microstructure formation. *Construction and Building Materials, 105*, 554–562. https://doi.org/10.1016/j.conbuildmat.2015.12.147

Hosseinzadeh, H., Salehi, A. M., Mehraein, M., & Asadollahfardi, G. (2023). The effects of steel, polypropylene, and high-performance macro polypropylene fibers on mechanical properties and durability of high-strength concrete. *Construction and Building Materials, 386*, Article 131589. https://doi.org/10.1016/j.conbuildmat.2023.131589

Ibrahim, M. A., Farhat, M., Issa, M. A., & Hassa, J. (2017). Effect of material constituents on mechanical and fracture mechanics properties of ultra-high-performance concrete. *ACI Materials Journal, 114*, 453–465. https://doi.org/10.14359/51689717

Jin, L., Zhang, R., Tian, Y., Dou, G., & Du, X. (2018). Experimental investigation on static and dynamic mechanical properties of steel fiber reinforced ultra-high-strength concretes. *Construction and Building Materials, 178*, 102–111. https://doi.org/10.1016/j.conbuildmat.2018.05.152

Lessly, S. H., Kumar, S. L., Jawahar, R., & Prabhu, L. (2020). Durability properties of modified ultra-high performance concrete with varying cement content and curing regime. *Materials Today: Proceedings, 45*, 6426–6432. https://doi.org/10.1016/j.matpr.2020.11.271

Li, J., Wu, Z., Shi, C., Yuan, Q., & Zhang, Z. (2020b). Durability of ultra-high performance concrete—a review. *Construction and Building Materials, 255*, Article 119296. https://doi.org/10.1016/j.conbuildmat.2020.119296

Li, X., Zhang, Y., Shi, C., & Chen, X. (2020a). Experimental and numerical study on tensile strength and failure pattern of high performance steel fiber reinforced concrete under dynamic splitting tension. *Construction and Building Materials, 259*, Article 119796. https://doi.org/10.1016/j.conbuildmat.2020.119796

Li, Y., Tan, K. H., & Yang, E. H. (2019). Synergistic effects of hybrid polypropylene and steel fibers on explosive spalling prevention of ultra-high-performance concrete at elevated temperature. *Cement and Concrete Composites, 96*, 174–181.

Li, Y., Yang, A., Sun, B., Yang, S., Wang, P., & Gao, B. (2024). Multifactor analysis and prediction modeling of flexural reliability of steel fiber reinforced concrete (SFRC) based on resistivity and air content. *The Journal of Building Engineering (JOBE), 98*, Article 111510. https://doi.org/10.1016/j.jobe.2024.111510

Lv, L. S., Wang, J. W., Xiao, R. C., Fang, M. S., & Tan, Y. (2021). Influence of steel fiber corrosion on tensile properties and cracking mechanism of ultra-high performance concrete in an electrochemical corrosion environment. *Construction and Building Materials, 278*, Article 122338. https://doi.org/10.1016/j.conbuildmat.2021.122338

Maglad, A. M., Mansour, W., Tayeh, B. A., Elmasry, M., Yosri, A. M., & Fayed, S. (2023). Experimental and analytical investigation of fracture characteristics of steel fiber-reinforced recycled aggregate concrete. *The International Journal of Concrete Structures and Materials, 17*, 74.

Matar, P. J., & Assaad, J. J. (2019). Concurrent effects of recycled aggregates and polypropylene fibers on workability and key strength properties of self-consolidating concrete. *Construction and Building Materials, 199*, 492–500. https://doi.org/10.1016/j.conbuildmat.2018.12.091

Matar, P., & Z'ehil, G. P. (2019). Effects of Polypropylene Fibers on the Physical and Mechanical Properties of Recycled Aggregate Concrete. *Journal of Wuhan University of Technology-Materials Science Edition, 34*(6), 1327–1344.

Mesbah Irandoost.F. (2010). S. A. Javadian Concrete technology and laboratory along with concrete mixing plan: in accordance with the national standard of Iran: 9th topic and (Aba) and (Det). Shahrashoob publisher, Tehran (in Farsi).

Miao, C., Mu, R., Tian, Q., & Sun, W. (2002). Effect of sulfate solution on the frost resistance of concrete with and without steel fiber reinforcement. *Cement and Concrete Research, 32*, 31–34. https://doi.org/10.1016/S0008-8846(01)00624-X

Nogueira, V., Taissum, D., & De Andrade, F. (2021). Creep mechanisms in precracked polypropylene and steel fiber-reinforced concrete. *Journal of Materials in Civil Engineering, 33*, 04021187.

Özbay, E., Erdemir, M., & Durmuş, H. İ. (2016). Utilization and efficiency of ground granulated blast furnace slag on concrete properties—a review. *Construction and Building Materials, 105*, 423–434. https://doi.org/10.1016/j.conbuildmat.2015.12.153

Richard, P., & Cheyrezy, M. (1995). Composition of reactive powder concretes. *Cement and Concrete Research, 25*, 1501–1511. https://doi.org/10.1016/0008-8846(95)00144-2

Russell, H. G. (1999). ACI Defines High-Performance Concrete. *Concrete International., 21*, 56–57.

Sharma, R., & Senthil, K. (2023). An investigation on mechanical and microstructural properties of hybrid fiber reinforced concrete with manufactured sand and recycled coarse aggregate. *The Journal of Building Engineering (JOBE), 69*, Article 106236. https://doi.org/10.1016/j.jobe.2023.106236

Shen, D., Liu, C., Kang, J., Yang, Q., Li, M., & Li, C. (2022). Early-age autogenous shrinkage and tensile creep of hooked-end steel fiber reinforced concrete with different thermal treatment temperatures. *Cement and Concrete Composites, 131*(2022), Article 104550.

Shen, P., Lu, L., He, Y., Wang, F., & Hu, S. (2019). The effect of curing regimes on the mechanical properties, nano-mechanical properties and microstructure of ultra-high performance concrete. *Cement and Concrete Research, 118*, 1–13. https://doi.org/10.1016/j.cemconres.2019.01.004

Shin, W., & Yoo, D.-Y. (2020). Influence of steel fibers corroded through multiple microcracks on the tensile behavior of ultra-high-performance concrete. *Construction and Building Materials, 259*, Article 120428. https://doi.org/10.1016/j.conbuildmat.2020.120428

Tahwia, A. M., Elgendy, G. M., & Amin, M. (2021). Durability and microstructure of eco-efficient ultra-high-performance concrete. *Construction and Building Materials, 303*, Article 124491. https://doi.org/10.1016/j.conbuildmat.2021.124491

Wang, J. Y., & Guo, J. Y. (2018). Damage investigation of ultra-high performance concrete under direct tensile test using acoustic emission techniques. *Cement and Concrete Composites, 88*, 17–28.

Wang, S., Xu, L., Chi, Y., Cui, K., Yin, C., & Li, B. (2023). Cyclic tensile behavior of ultra-high performance concrete with hybrid steel-polypropylene fiber: Experimental study and analytical model. *Composite Structures, 321*, Article 117255.

Wu, Z., Khayat, K. H., & Shi, C. (2019a). Changes in rheology and mechanical properties of ultra-high-performance concrete with silica fume content. *Cement and Concrete Research, 123*, Article 105786. https://doi.org/10.1016/j.cemconres.2019.105786

Wu, Z., Khayat, K. H., & Shi, C. (2019b). Changes in rheology and mechanical properties of ultra-high performance concrete with silica fume content. *Cement and Concrete Research, 123*, Article 105786. https://doi.org/10.1016/j.cemconres.2019.105786

Wu, Z., Shi, C., & Khayat, K. H. (2016). Influence of silica fume content on microstructure development and bond to steel fiber in ultra-high strength cement-based materials (UHSC). *Cement and Concrete Composites, 71*, 97–109. https://doi.org/10.1016/j.cemconcomp.2016.05.005

Xie, T., Fang, C., Mohamad Ali, M. S., & Visintin, P. (2018). Characterizations of autogenous and drying shrinkage of ultra-high performance concrete (UHPC): An experimental study. *Cement and Concrete Composites, 91*, 156–173. https://doi.org/10.1016/j.cemconcomp.2018.05.009

Yoo, D. Y., & Kim, M. J. (2019). High energy absorbent ultra-high-performance concrete with hybrid steel and polyethylene fibers. *Construction and Building Materials, 209*, 354–363.

Yu, R., Spiesz, P., & Brouwers, H. (2014b). Mix design and properties assessment of ultra-high performance fiber reinforced concrete (UHPFRC). *Cement and Concrete Research, 56*, 29–39. https://doi.org/10.1016/j.cemconres.2013.11.002

Yu, R., Tang, P., Spiesz, P., & Brouwers, H. J. H. (2014a). A study of multiple effects of nano-silica and hybrid fibers on the properties of Ultra-High Performance Fibre Reinforced Concrete (UHPFRC) incorporating waste bottom ash (WBA). *Construction and Building Materials, 60*, 98–110. https://doi.org/10.1016/j.conbuildmat.2014.02.059

Publisher's Note

Shiva Safari Taleghani Former M.Sc. Student, Department of Civil Engineering, Kharazmi University, Iran.

Amir Masoud Salehi Assistant Professor, Department of Civil Engineering, Kharazmi University, Iran.

Mojtaba Mehraein Associate Professor, Department of Civil Engineering, Kharazmi University, Iran.

Gholamreza Asadollahfardi Professor Emeritus, Department of Civil Engineering, Kharazmi University, Iran.